CHALMERS

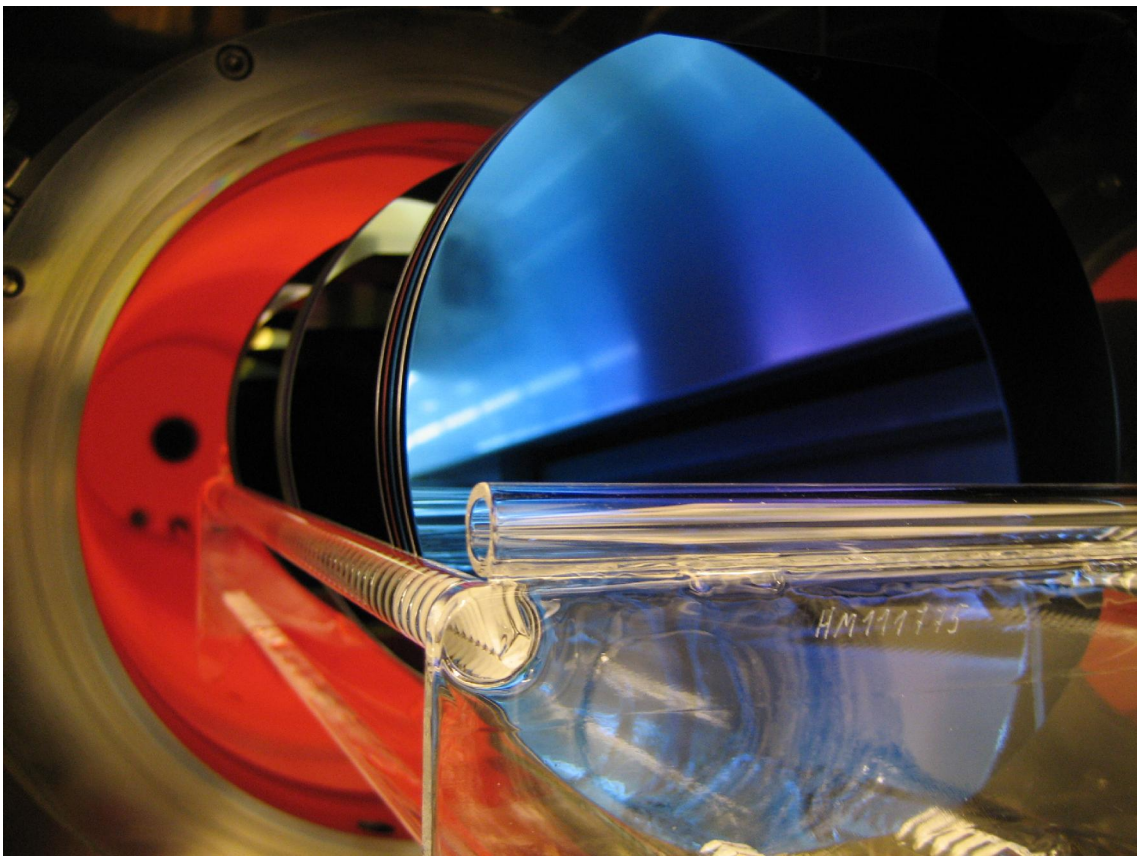

Optimisation and characterisation of LPCVD silicon nitride thin film growth

Master of Science Thesis

SOFIA TÖNNBERG

Department of Microtechnology and Nanoscience
Nanofabrication Laboratory
CHALMERS UNIVERSITY OF TECHNOLOGY
Göteborg, Sweden, 2006

Optimisation and characterisation of LPCVD silicon nitride thin film growth

Sofia Tönnberg

Department of Microtechnology and Nanoscience
Nanofabrication Laboratory
Chalmers University of Technology

Examiner:
Jan Stake

Supervisor:
Örjan Arthursson

Göteborg 2006

ISSN 1652-0769
Technical Report – MC2 54

Cover:
Silicon wafers with a thin layer of deposited silicon nitride, shown during the unload process from a Centrotherm LPCVD horizontal furnace (MC2 tool No. 708.3).

Abstract

In this master thesis project a Low Pressure Chemical Vapor Deposition (LPCVD) furnace was used to deposit thin (100-200 nm) silicon nitride films onto silicon wafers. Twelve different runs were performed, each with a specific set of values for different deposition parameters. The parameters in question were dichlorosilane (DCS) to ammonia (NH_3) ratio, total flow, pressure, and temperature.

Analysis of the properties of these films where then made by the use of ellipsometry, atomic force microscopy (AFM), and stylus profilometry. From the obtained results, conclusions could be made of how different deposition parameters affect film properties such as deposition rate, refractive index, thickness uniformity over a wafer, roughness, and stress. The most desired properties were low stress and low roughness. The analysis revealed that it was difficult to achieve this goal, and suggests the following combination of parameters for a result as close as possible to the desired: T = 770 °C, p = 150 mTorr, DCS:NH_3 ratio = 3:1, total flow = 200 sccm.

Prior to the laboratory work, an initial literature study of papers regarding similar subjects was conducted. This provided clues to the range of interest to use for the deposition parameters in this project.

Acknowledgements

This thesis work has been carried out at the Department of Nanoscience and Microtechnology (MC2), Nanofabrication Laboratory. It has been a great experience for me to work in an environment such as the cleanroom facility at this department. Not only because I have gained so much knowledge about this kind of work in general, but also because it has been fascinating to use the kind of equipment in practice, which I only had heard mentioned or learnt about in theory during my undergraduate studies. I would especially like to thank my supervisor Mr. Örjan Arthursson for all help and education regarding the equipment, and also for valuable discussions during the whole process.

I would also like to thank Mr. Thomas Wagner, L.O.T.-Oriel GmbH & Co. KG, Darmstadt, for help regarding analysing the data from the ellipsometry measurements, and Mr. Uwe Höhne, Centrotherm GmbH & Co. KG, Hannover, for providing suggestions on parameter ranges for the LPCVD furnace.

Göteborg, January 2006

Sofia Tönnberg

Table of content

1 Introduction

1.1 Background

Fabrication processes of microelectronic devices involve many steps in which thin films of various materials are deposited on the surface of a silicon wafer. Examples of different materials that are deposited include metals, amorphous silicon and polysilicon, and dielectrics such as silicon dioxide and silicon nitride.

Methods for depositing these films can be divided into two groups: Physical Vapor Deposition (PVD) and Chemical Vapor Deposition (CVD). Two of the methods that belong to the first group, i.e. do not involve chemical reactions, are evaporation and sputtering. Instead, they produce a vapor of the material to be deposited by heating, in the case of evaporation, or by energetic ion bombardment, in the case of sputtering. They are mostly used for depositing metal films. For deposition of semiconducting or insulating films it is more common to use methods from the second group, i.e. methods based on chemical reaction processes. While evaporation and sputtering require vacuum systems operating at low pressure, CVD can be performed at either reduced or atmospheric pressure (not for silicon nitride, this deposition only occurs at low pressure). There are also modifications of simple thermal CVD processes that provide alternative energy sources, allowing the deposition to occur at low temperature. Examples are the use of plasmas or optical excitation to drive the chemical reactions.

1.2 Purpose

The cleanroom facility at the Department of Nanoscience and Microtechnology (MC2), Chalmers University of Technology, is equipped with a 4-stack Low Pressure Chemical Vapor Deposition (LPCVD) furnace, capable of depositing silicon nitride, poly-crystalline silicon, or amorphous silicon, and silicon dioxide (TEOS and LTO, i.e. oxide based on TetraEthylOrthoSilicate and Low Temperature Oxide based on silane). The goal of this project was to find out how different deposition parameters like temperature and pressure influence the properties of deposited silicon nitride films onto silicon wafers.

The most important properties to examine are the roughness and the intrinsic stress in the film, because low roughness and low stress are required in many applications. It is for example well known that both surface roughness and internal stresses of thin films have a major influence on the quality of wafer bonding processes used in MEMS (MicroElectroMechanical Systems) processing [P1].

So, besides finding out in general how different deposition parameters influence the properties of a thin silicon nitride film, part of the goal was also to try to find an ideal composition of different deposition parameters that would provide a silicon nitride layer with these desired properties of low stress and low surface roughness.

This goal was to be obtained through an initial literature study of previous work regarding the same subjects. After this literature study, several depositions were to be made, and finally

analysis of the deposited films would provide results from which relevant conclusions could be made.

2 Chemical vapor deposition methods

As mentioned in the introduction, Chemical Vapor Deposition, or CVD for short, is a technique used in thin film manufacturing. It is used for depositing materials like polysilicon, amorphous silicon, silicon nitride or silicon dioxide. Besides deposition of dielectric materials, CVD is also used for depositing different metals such as tungsten (W). The common factor for deposition of these different materials by CVD is that the coatings are conformal, have good step coverage, and can coat a large number of wafers at the same time [B1]. The method is based on thermal decomposition and/or reaction of gaseous compounds, and the desired material is deposited directly from the gas phase onto the surface of a substrate.

Some of the advantages with CVD are that it can be performed at pressures high enough for which the mean free path for gas molecules is quite small, and the use of relatively high temperatures. It is these high temperatures that can provide excellent conformal step coverage over a broad range of topological profiles [B2].

There are a number of CVD variations used for depositing these thin films. Three of the most common are presented in further detail in the subsections below: Low Pressure CVD (LPCVD), see section 2.1, Atmospheric Pressure CVD (APCVD), section 2.2, and Plasma Enhanced CVD (PECVD), section 2.3. When making the choice between these different deposition methods several things have to be considered: the substrate temperature, the deposition rate and film uniformity, the morphology, the electrical and mechanical properties, and the chemical composition of the films.

2.1 Low Pressure CVD

A variety of system geometries have been used for LPCVD. These systems can be divided into two different categories: hot and cold wall systems. Hot wall systems have the advantages of uniform temperature distributions and reduced convection effects. Cold wall systems are able to reduce deposition on the walls. These deposits can lead to depletion of the deposition species and the formation of particles, which may flake off the walls and fall on the wafers. Deposits on the walls also lead to memory effects, i.e. the deposition on the wafer of material previously deposited on the walls. For that reason hot wall reactors must be dedicated to the growth of a particular film [B3].

A hot-wall, LPCVD system is shown in Figure 2.1. It is commonly used to deposit poly-silicon, silicon dioxide and silicon nitride. In this example, the reactant gases are introduced into one end of a multi-zone furnace tube, and are pumped out the other end. This common use of 2 or more independently controlled heating zones allows some control of the axial temperature along the reactor.

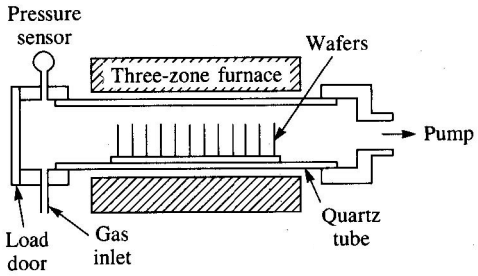

Figure 2.1: Three-zone furnace tube hot-wall LPCVD system [B2].

Temperature range is from 300 °C to 1150 °C [B2], with typical values being between 700 °C and 800 °C [I1]. An example of a typical deposition rate is around 10 nm/minute, a low value compared with the 100 nm/minute of APCVD (section 2.2). Even so, because many applications employ very thin films, throughput is reasonable in batch processing. Advantages with LPCVD systems are that several hundred wafers may be processed in a single run, and excellent uniformity can be obtained. Hot-wall systems have the disadvantage that the tube must be periodically cleaned or replaced to minimise problems with particle matter, because the deposited film simultaneously coats the inside of the tube.

The horizontal LPCVD systems are generally built in stacks of three to four tubes (compare Figure 5.1, section 5.1). The gasses are controlled at the back of the tube using mass flow controllers and routed to the front of the furnace. The gasses are either injected through a ring at the front of the tube, or they can be connected to a tube that runs the length of the furnace and injects gasses uniformly across the wafers. Most production systems have soft landing loaders or cantilevers. This will hopefully minimise particle formation and flaking during the load/unload process.
When the loading is finished, the furnace is closed with an O-ring-sealed door. Then, the tube is flushed with an inert gas such as N_2 and pumped to a medium vacuum. If the furnace is not already idling at the deposition temperature, that temperature is reached through a ramping procedure, after which the deposition gases are finally switched on. The deposition is allowed to proceed for a predetermined time, and then the furnace is again flushed with N_2. The wafers are unloaded after the pressure has been raised back to atmospheric pressure.

A more recent innovation in the LPCVD area is the introduction of vertical furnaces [B3]. In these systems, the wafers are all held by gravity. This gives an advantage over standard tubes, since the wafer-to-wafer spacing in the reactor is more uniform. Also, convective effects are more uniformly distributed across the wafer. Because of these advantages, vertical LPCVD systems can routinely achieve non-uniformities of better than 2% in the deposition of for example silicon nitride. Vertical CVD systems are more easily integrated into automated factories since the wafers do not have to be tipped to the vertical, which allows easier robotic handling. There is one final advantage that is very important, and that is reduced particle counts. However, compared with conventional LPCVD systems these vertical chambers also have a disadvantage, the cost of these newer systems being considerably higher.

2.2 Atmospheric Pressure CVD

APCVD is known for its high reaction rates and simplicity as a CVD system, particularly for the deposition of dielectrics. Therefore, some of the earliest CVD processes were done at atmospheric pressure. Because of high deposition rates, in excess of 100 nm/min, it is now most commonly used for deposition of thick dielectrics. For thin layers, LPCVD systems are preferred since they provide much better uniformity of the deposited films [B3].

Figure 2.2 shows an example of a simple APCVD reactor, in this case a continuous reactor. This type of reactor is often used for deposition of a silicon dioxide passivation layer as one of the last steps in integrated circuit processing. The reactant gases flow through the center section of the reactor and are confined by nitrogen curtains at the ends. Wafers travel from cassette to cassette on a heated chain track. The gases are injected from a showerhead above the wafers.

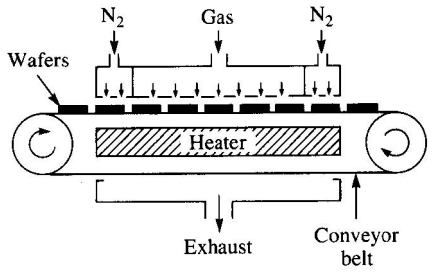

Figure 2.2: Continuous atmospheric pressure CVD reactor [B2].

The substrates can be fed continuously through the system, and large-diameter wafers are easily handled. A disadvantage with this type of reactor is that high gas-flow rates are required. Temperatures may vary from 240 °C to 450 °C.

A major drawback of APCVD, besides low uniformity, is particle formation. This is especially a problem for this kind of continuous reactor. Adding a sufficient amount of N_2 or another inert gas can control particle formation in the gas phase. But there is also a problem with deposition that occurs at the gas injectors. Even if the growth rate of these particles is low, after a number of wafers the particles will become large enough to flake off and fall on the wafer surface. To avoid this problem, the showerhead may be segmented so as to keep the reactant gasses separated until they are injected into the chamber.

2.3 Plasma Enhanced CVD

Chemical vapor deposition can also take place in a plasma reactor. Because of the formation of a plasma, the reaction is allowed to take place at low temperatures, typically between 250 °C to 400 °C [I2]. This is because the plasma is an alternative energy source for the gaseous and/or adsorbed molecules. A plasma is a partially ionized gas, which can be used in place of high temperature to crack molecules and so drive some reaction chemistry. It may also be

used to create and accelerate ions. PECVD systems have the added advantage of using ion bombardment of the surface to provide energy to the adspecies to allow them to diffuse further along the surface, without a high substrate temperature. As a result, the process is very good at filling small features.

Figure 2.3 shows a simple parallel plate plasma reactor. Two parallel plates are contained in a vacuum system and a high voltage source is connected to a dc supply through vacuum power feedthroughs.

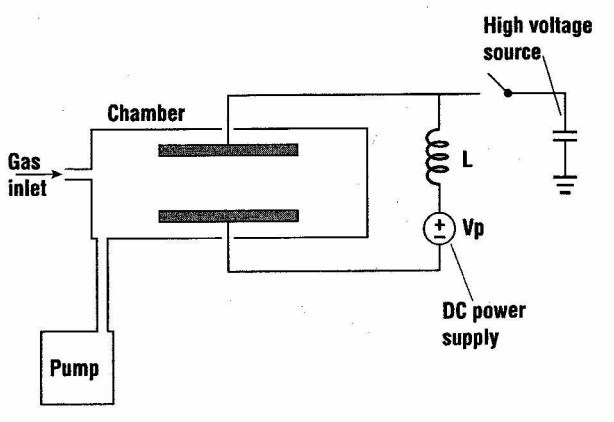

Figure 2.3: Parallel plate plasma reactor [B3].

A typical pressure for a plasma process is 1 Torr. A high voltage source is connected momentarily to the circuit to start the plasma. When the material on one or more electrodes is insulating, the electric field created by the conducting gas will be reduced. This is due to charge accumulation on the surface of the insulating material, and the reduction of the field will lead to that the plasma is ultimately extinguished. To solve this problem, the plasma can be driven by an ac-signal. Sources are in the radio frequency (RF) range, so this is a so-called RF plasma system [B3].

Figure 2.4 shows a parallel-plate PECVD system. In this system, the wafers lie on a grounded aluminium plate which serves as the bottom electrode for establishing the plasma. The wafers can be heated up to 400 °C by using high-intensity lamps or resistance heaters. A second aluminium plate, placed in close proximity to the wafer surface, serves as the top electrode.

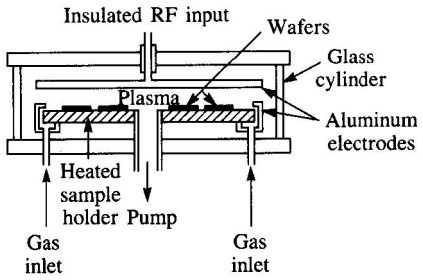

Figure 2.4: Parallel-plate PECVD system [B2].

Gases are introduced along the outside of the system, flow radially across the wafers, and are pumped through an exhaust in the centre. Wafers must be loaded manually, and the capacity of the system is also limited. A major problem when it comes to VLSI (Very Large Scale Integration) fabrication is that particles may fall from the upper plate onto the wafers.

To be able to handle a larger number of wafers at one time, it is better to use a three-zone furnace tube, much like the one described in section 2.1 for LPCVD. This type of furnace is shown in Figure 2.5. A special electrode assembly holds the wafers parallel to the gas flow. The plasma is established between alternating groups of electrodes supporting the wafers.

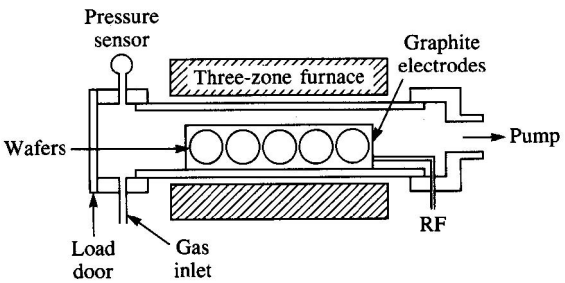

Figure 2.5: Three-zone furnace tube PECVD system [B2].

Besides the advantage of a lower deposition temperature than for LPCVD, there is also another part to take into consideration. PECVD offers a special way to reduce the high stress that is often present in silicon nitride films. In plasma deposition, ion bombardment can be used for densification of films, which makes them more compressive, thus reducing the high tensile stress [I2]. (For an explanation of tensile and compressive stress, see Figure 4.4, section 4.4.)

There are also different kinds of PECVD, one being the so-called ICP PECVD. ICP stands for Inductively Coupled Plasma, and in this type of plasma source the energy is supplied by electrical currents which are produced by electromagnetic induction. Compared with a conventional PECVD process, ICP allows control of more process parameters.

3 Silicon Nitride

This section connects the content of section 2 to the material of interest in this project: silicon nitride. Section 3.1 describes how silicon nitride is deposited with different kinds of CVD, while section 3.2 points at the applications of these films. Also, a short description of sputtering is given in section 3.1 together with some properties of silicon nitride deposited with this method. This is included to provide some comparative information from a PVD method.

3.1 Deposition

3.1.1 CVD

It is difficult to grow silicon nitride by thermal nitridation, e.g. with ammonia, because of its low growth rate and high growth temperature. Silicon nitride will form when silicon is exposed to ammonia at temperatures between 1000 °C and 1100 °C, but the growth rate is very low.

However, silicon nitride films can be deposited both through reactions between silane (SiH_4) and ammonia (NH_3), and through reactions between dichlorosilane ($SiCl_2H_2$) and ammonia, under different process conditions. The silane reaction can occur between 700 °C and 900 °C at atmospheric pressure according to the reaction formula:

$$3SiH_4 + 4NH_3 \rightarrow Si_3N_4 + 12H_2.$$

Dichlorosilane is instead used in an LPCVD system, usually between 700 °C and 800 °C. The reaction is described through the reaction formula:

$$3SiCl_2 + 4NH_3 \rightarrow Si_3N_4 + 6HCl + 6H_2.$$

In plasma systems, silane will react with a nitrogen discharge to form plasma nitride (SiN), according to:

$$2SiH_4 + N_2 \rightarrow 2SiNH + 3H_2.$$

(The H in SiNH indicating a high content of hydrogen in the film.)

Silane will also react with ammonia in an argon plasma:

$$SiH_4 + NH_3 \rightarrow SiNH + 3H_2.$$

LPCVD films are often hydrogen-rich, containing up to 8 % hydrogen. Plasma deposition does not produce stoichiometric silicon nitride films. Instead, the films contain as much as

20 % to 25 % hydrogen [B2]. LPCVD films usually have high internal tensile stresses, and films thicker than 200 nm may crack because of this stress. On the other hand, plasma-deposited films often have lower tensile stresses (an explanation of this was given in section 2.3).

The resistivity (10^{16} Ω-cm) and dielectric strength (10 MV/cm) of the LPCVD nitride films are better than those of most plasma films. Resistivity of plasma nitride can range from 10^{5} Ω-cm to 10^{21} Ω-cm, depending on the amount of nitrogen in the film, while the dielectric strength ranges between 1 MV/cm and 6 MV/cm [B1].

3.1.2 Sputtering

Unlike CVD, the sputtering process is not thermally activated. A description of this physical process is given in Figure 3.1. A solid surface is bombarded with energetic particles such as accelerated ions, whereby surface atoms of the solid are scattered due to collisions between the surface atoms and the energetic particles. These scattered surface atoms are then deposited onto a substrate.

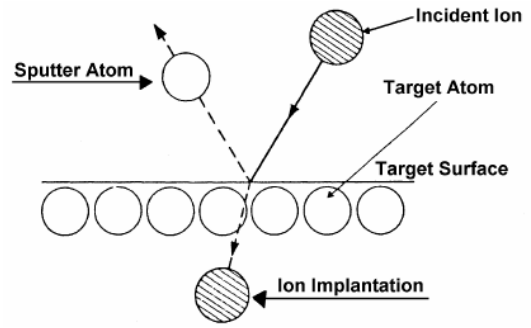

Figure 3.1: The physical sputtering processes [B4].

One form of sputtering is cathode sputtering, which is commonly used for depositing thin films. The basic principle of the simplest model, the dc diode sputtering system, is illustrated in Figure 3.2. A cathode is bombarded by ions from the plasma set up between two plates, and cathode atoms are scattered from the metal surface. These atoms are then deposited onto a substrate placed on the anode. The sputtering gas is typically argon gas at a pressure of 40 mTorr [B4].

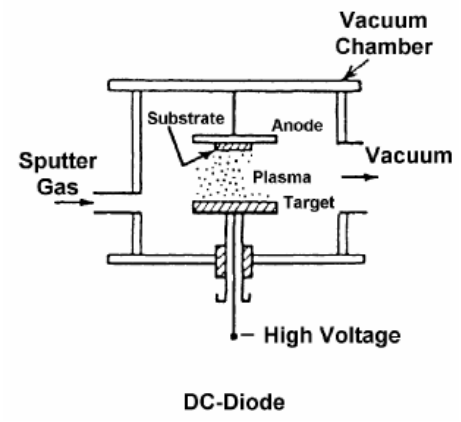

Figure 3.2: Illustration of a dc diode sputtering system [B4].

Another cathode sputtering system, often used for silicon nitride deposition, is magnetron sputtering. In this method, a magnetic field is superposed on the cathode and glow discharge. Due to an increased collision rate between the electrons and the sputtering gas atoms or molecules, a lower pressure can be used. Also, an increased plasma density leads to an increased sputtering rate at the target. Due to the low pressure, the risk of collision between the sputtered particles and the particles in the gas will be minimised, resulting in a higher deposition rate.

To sputter insulators, radio frequency sputtering is required (compare the discussion of PECVD, section 2.3).

A comparison of typical deposition conditions for silicon nitride, between PECVD and magnetron sputtering (MSP), is given in Figure 3.3. Sputtering uses a lower temperature and has a lower deposition rate.

Materials	Structure*	Deposition Method	Substrate	Deposition Conditions			Film Properties
				Substrate Temp. (°C)	Dep. Rate (μm/hr)	Misc.	
Si_3N_4	a	P-CVD	Si	250	3	reaction gas: $N_2 + NH_3 + SiH_4$	$n_0 \approx 2.0–2.1$ (6328 Å)
	a	RF-MSP	Si	100	1	Si_3N_4 target: Ar	$n_0 \approx 2.1$ (6328 Å)

* a = amorphous

Figure 3.3: Deposition conditions for silicon nitride [B4].

3.3 Applications

Silicon nitride is a material that has excellent overall properties such as [B5]:

- Light weight.
- High strength and toughness (for a ceramic material).
- High chemical resistance to acids, bases, salts, and molten metals.
- Good resistance to oxidation up to 1500 ºC.
- High electrical resistivity.

It is a dielectric material, and as such it is important in applications regarding integrated circuit devices. Dielectric films are used mainly for insulation and passivation, both for discrete devices and integrated circuits. For instance, LPCVD silicon nitride films are often used for passivation, since they serve as good barriers to the diffusion of water and sodium. In fact, silicon nitride is an excellent barrier to just about everything, and it is often used as a hard mask for wet and dry etching. The films can also be used as masks for the selective oxidation of silicon because silicon nitride oxidizes very slowly and prevents the underlying silicon from oxidizing. Plasma-deposited nitride provides excellent scratch protection, serves as a moisture barrier, and prevents sodium diffusion [B1].

Usually, a deposited nitride has a very high tensile stress of a few GPa, but a more silicon rich film has a lower stress, typically down to a few hundred MPa. To have a low stress is very important in most cases, it is a prerequisite for example for manufacturing of thin windows of the material. With a high stress, these would crack and shatter. These thin windows are used for many different purposes, for instance as substrates in Rutherford Back Scattering experiments (as thin as 20 nm) or as transmissive windows in infrared light, extreme ultra-violet light, and x-ray experiments (100 nm) [I3].

The films also have a good mechanical strength, which together with the strong resistance to many etchants make the silicon nitride films interesting for use in MEMS fabrication [I4].

There is also an interest for composite films of oxide and nitride. These are used as very thin gate insulators in scaled VLSI devices, and they are also used as the gate dielectric in electrically programmable memory devices [B2].

4 Methods of analysis and etching

In this project some different techniques for analysing the deposited silicon layer were used. This section presents some relevant background information concerning these techniques and also a short description about plasma etching, which was used during the laboratory work. The different techniques are displayed in the order of usage: ellipsometry is presented in section 4.1, scanning probe microscopy in section 4.2, plasma etching is described in section 4.3, while an explanation of profilometry is given in section 4.4.

4.1 Ellipsometry

Ellipsometry is an optical technique for surface, thin film and multilayer characterization, but it is also suitable for studies of dynamic surface phenomena like macromolecular adsorption. It is based on oblique reflection of incident polarized light at a surface, and the method consists of measuring the change in the polarization state when the beam is reflected from the surface [B6] [B7]. An illustration of this is given in Figure 4.1.

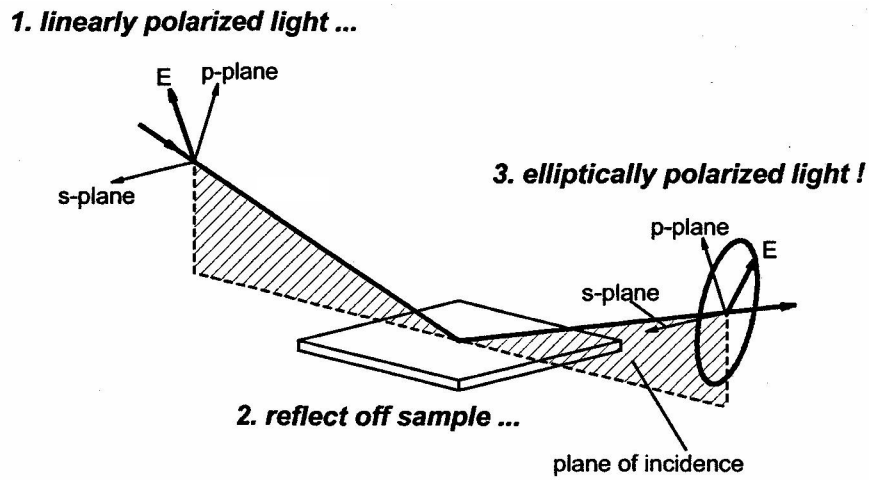

Figure 4.1: Geometry of an ellipsometric experiment, showing the parallel (p) and perpendicular (s) directions [B8].

Because of different reflection conditions when the angle of incidence is non-zero, the polarization components parallel and perpendicular to the plane of incidence must be distinguished. So, the basic quantity measured in ellipsometry is the overall complex reflectance ratio, which is defined as:

$$\rho = \frac{R_p}{R_s} = \left|\frac{R_p}{R_s}\right| e^{i(\partial_p - \partial_s)},$$

where R_p is the parallel component of the total Fresnel reflection coefficient (calculated based on a three-phase model in the case of a thin film on a substrates), R_s is the perpendicular component, and ∂_p and ∂_s are their phases.

It can also be expressed in polar form as:

$$\rho = \tan\psi e^{i\Delta},$$

where the amplitude ratio is: $\tan\psi = \left|\frac{R_p}{R_s}\right|$,

and the phase difference is: $\Delta = \partial_p - \partial_s$.

These two parameters, ψ and Δ, are called the ellipsometric angles. The difference in amplitude and phase between the electric field in the two polarization directions can be measured very accurately, thus enabling film thickness down to small fractions of the wavelength of the incident light to be measured. That is, sub-Ångström resolution in film thickness can readily be obtained. The method is contactless and non-destructive. It also has an advantage compared to other optical techniques, such as transmission and reflectance measurements: there is no need to measure the absolute intensity of the light.

When using ellipsometry, the measured quantities, which in general are functions of wavelength and angle of incidence and polarization state, have in most cases no direct meaning in the analysis of a sample. The measured quantities must be evaluated to extract the optical properties and film thickness of interest. This means that ellipsometry is an indirect method. The evaluation is accomplished by the construction of a model from which the parameters of interest can be predicted. By varying the unknown physical parameters defining the model, e.g. optical constants and thickness, the calculated model data is made to match the measured data as closely as possible, through an iterative procedure. If then an acceptable fit is obtained, the model hopefully will represent the true physical structure of the sample under study.

For a dielectric material, such as silicon nitride, a useful model involves a so-called Cauchy layer [B8]. This is a function based layer, which means that it derives its optical constants from a mathematical expression instead of the more common wavelength-by-wavelength tables. For instance, over part of the spectral range, the index of refraction can be represented by a slowly varying function of wavelength, λ, according to the formula:

$$n(\lambda) = A + \frac{B}{\lambda^2} + \frac{C}{\lambda^4}.$$

Each of the parameters A, B, C, can be defined as a variable fit parameter.

To check if an acceptable fit has been obtained, a value called the mean square error (MSE) is given. MSE states how well the calculated curve from the model matches the measured graph, and it is calculated as:

$$\mathrm{MSE} = \sqrt{\frac{1}{2N-M}\sum_{i=1}^{N}\left[\left(\frac{\psi_i^{\mathrm{mod}}-\psi_i^{\mathrm{exp}}}{\sigma_{\psi,i}^{\mathrm{exp}}}\right)^2+\left(\frac{\Delta_i^{\mathrm{mod}}-\Delta_i^{\mathrm{exp}}}{\sigma_{\Delta,i}^{\mathrm{exp}}}\right)^2\right]}.$$

The number of measured ψ and Δ pairs is N, and the total number of real valued fit parameters is M.

4.2 Scanning Probe Microscopy

Scanning Probe Microscopy (SPM) is the collective name for different microscopy forms where a sharp probe is scanned across a surface and some interaction/interactions between the probe and the sample are monitored. The two primary forms of SPM are Scanning Tunneling Microscopy (STM) and Atomic Force Microscopy (AFM, also called Scanning Force Microscopy). While STM is based on the fact that the tunneling current between a conductive tip and sample is exponentially dependent on their separation, AFM is instead based on the atomic force (i.e. van der Waals forces) between the tip and the sample. In this project, AFM was used. There are also three different primary modes of AFM: contact mode, non-contact mode and tapping mode AFM. The technique used here is the tapping mode, which can be described in short as:

The basics of tapping mode AFM is illustrated in Figure 4.2. It operates by scanning a tip attached to the end of an oscillating cantilever across the sample surface. During scanning, the tip lightly “taps” on the sample surface, contacting the surface at the bottom of its swing.

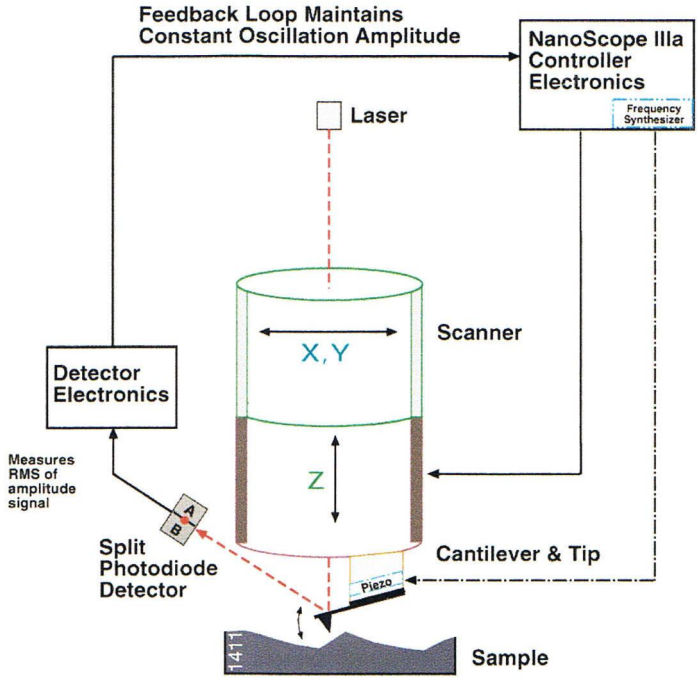

Figure 4.2: Illustration of the basics of tapping mode AFM [B9].

A feedback loop maintains a constant oscillation amplitude by maintaining a constant RMS of the oscillation signal acquired by a split photodiode detector. A topographic image of the sample surface is created through the storage of the vertical position of the scanner at each (x,y) data point in order to maintain a constant "setpoint" amplitude.

There are several different ways in which the topographic image can be analysed. For example, roughness measurements can be performed either over the entire image or a selected portion of the image. Results from these measurements are displayed as different roughness parameters, two of the most common ones being R_a and RMS (Rq). R_a is the mean roughness and represents the arithmetic average of the deviations from the centre plane. It is calculated as:

$$R_a = \frac{\sum_{i=1}^{N} \left| Z_i - Z_{cp} \right|}{N},$$

where Z_{cp} is the value of the centre plane, Z_i is the current Z value, and N is the number of points within a given area. RMS is the root mean square roughness and represents the standard deviation of the Z values within a given area. It is used more often than the R_a value in the literature, and is defined as:

$$\text{RMS} = \sqrt{\frac{\sum_{i=1}^{N}(Z_i - Z_{ave})^2}{N}},$$

where Z_{ave} is the average Z value within the given area, Z_i is the current Z value, and N is the number of points within a given area.

Besides these measurements, it is also useful to display the topographical image by the method of PSD (power spectral density) [P2]. This is because R_a and RMS values only gives average values of the variations in the topography and do not show the true height of individual "spikes" in the surface. As an example, imagine a surface with many small spikes and another surface with a few very large spikes. These two surfaces could show about the same R_a or RMS values, but the surface with the very large spikes might be of no use for a specific application. PSD provides a representation of the amplitude of a surface's roughness as a function of the spatial frequency, or wavelength, of the roughness. This means that the PSD function gives a graphical representation of how periodic surface features are distributed. This may for instance reveal some characteristics of the material such as grains. To compare topographical images, it is common to use 2D isotropic PSD. As the name indicates, this is a two-dimensional power spectral density. It has the unit of 1 over area squared, which is length to the fourth power (here: $1/\text{nm}^4$). It is isotropic in the sense that it is an average taken over all directions in the data.

The frequency distribution for a digitized profile of length L, consisting of N points sampled at intervals of d_0 is approximated by [B10]:

$$\text{PSD(f)} = \frac{2d_0}{N}\left|\sum_{n=1}^{N} e^{\frac{i2\pi}{N}(n-1)(m-1)} z(n)\right|^2 \quad , \quad \text{for f} = \frac{m-1}{Nd_0},$$

where frequencies, f, range from $\frac{1}{L}$ to $\frac{N/2}{L}$. So, the algorithm used to obtain the PSD depends upon squaring the FFT (Fast Fourier Transform) of the image to derive the power. Once the power, P, is obtained, it may be used to derive the 2D isotropic PSD as:

$$\text{2D isotropic PSD} = \frac{P}{2\pi f(\Delta f)}$$

The RMS roughness value is actually the square root of the integral of the PSD, over some wavelength or frequency interval. Even so, additional information can be obtained when comparing the shape of two PSD curves from different wafers with about the same RMS roughness values. For example, a slower variation over the wavelength suggests a larger lateral structure (grain size). See Figure 4.3.

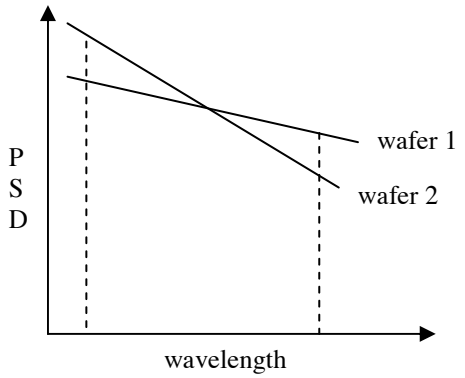

Figure 4.3: Illustration of PSD curves for two different wafers. The integrals of the PSD, i.e. the areas under the curves, will be the same, resulting in the same RMS roughness values. Even so, the slower variation over the wavelength for wafer number 1 gives the additional information that the surface of this wafer has a larger grain size.

4.3 Plasma Etching

Etching in a plasma environment has several significant advantages when compared with wet etching. During wet etching, wafers are immersed in a solution that reacts with the exposed film to form soluble by-products. This process is difficult to control. Not only because the by-products can have an influence on the etch rate, but also since they can affect the result through changing the anisotropy and the roughness. Also, wet etching often has high defect levels due to solution particle contamination, cannot be used for small features (because of under etching), and produces large volumes of chemical waste.

Plasmas, on the other hand, are much easier to start and stop than simple immersion wet etching. Plasma etch processes are also much less sensitive to small changes in the temperature of the wafers. These two factors make plasma etching more repeatable than wet etching. Most importantly for small features, plasma etches may have high anisotropies, i.e. only a small lateral etch rate compared with the vertical etch rate. Plasma environments may also have far fewer particles than liquid media. Finally, a plasma etch process produces less chemical waste.

As in the case of plasma enhanced CVD (section 2.3), the wafer is placed directly onto one of the electrodes that establish the plasma. For a plasma etch process to proceed, six steps must occur [B3]. A feed gas introduced into the chamber must be broken down into chemically reactive species by the plasma. These species must diffuse to the surface of the wafer and be adsorbed. Once on the surface, they may move about (surface diffusion) until they react with the exposed film. The reaction product must be desorbed, diffused away from the wafer, and be transported by the gas stream out of the etch chamber.

In a typical plasma etch process, the surface of the film to be etched is subjected to an incident flux of ions, radicals, electrons, and neutrals. Although the neutral flux is by far the largest, physical damage is related to the ion flux. Chemical attack depends on both ion flux and the radical flux.

One example of a plasma etch process is Reactive Ion Etching (RIE), sometimes called ion-assisted etching, which has high anisotropy and high selectivity. The basic idea consists of

increasing the energy of the ion bombardment through increasing the potential difference from the plasma to the powered electrode. In a parallel-plate reactor this is done through attaching the neutral electrode to the chamber wall to enlarge its effective area. For this arrangement to be effective, the plasma must contact the chamber walls. If the pressure increases, the plasma contracts and loses contact with the walls. Therefore, RIE is done in a low-pressure plasma, since the mean free path in the plasma in this case is at least of order millimetres. Then the plasma remains in good contact with the walls.

4.4 Profilometry

Before presenting the basics around profilometry, here is a short description about the kinds of stress that are possible:
Stress in thin films results either from differences in thermal expansion (thermal stress) or from the microstructure of the deposited film (intrinsic stress). Thermal stress occurs in the cases when film depositions are made above room temperature. When the substrate together with the deposited film afterwards is cooled down from the deposition temperature to room temperature, differences in the thermal expansion coefficients of the substrate and the film cause thermal stress. Intrinsic stress results from the microstructure created in the film as atoms are deposited on the substrate.

The obtained stress can be either compressive or tensile. These expressions are explained in Figure 4.4. Figure 4.4a shows tensile stress, while Figure 4.4b demonstrates compressive stress.

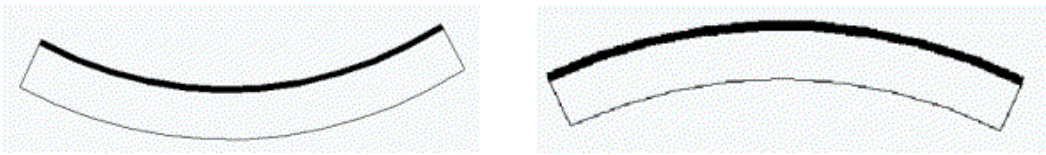

Figure 4.4: a) Tensile stress, conceptual diagram [I5]. The film wants to be "smaller" than the substrate because it was "stretched" to fit.

b) Compressive stress, conceptual diagram [I5]. The film wants to be "larger" than the substrate, because it was "compressed" to fit.

Tensile stress results from microvoids in the thin film, because of the attractive interaction of atoms across the voids. Compressive stress results when heavy ions or energetic particles strike the film during deposition. The impacts are like hitting the film with a hammer, packing the atoms more tightly.

A profilometer is a useful equipment for calculating stress in a thin film. It provides a tool for measuring the wafer curvature at the wafer surface. As was shown in Figure 4.4 above, besides providing figures for calculating the magnitude of the stress, these measurements also gives the answer to what kind of stress that is dominating in the film: tensile or compressive. The stress measurements are accomplished by creating a reference scan before deposition, and

comparing it with a post deposition scan of the same wafer (after the layer on one side of the wafer has been etched off with plasma etching), in the same position, using the same scan recipe. Because a stress recipe consists of scan length, scan speed, and sampling rate, placing the wafer in the same position as in the pre scan gives a comparable new measurement of the same scanned part as before deposition.

As a profile is taken, the height of the wafer is being measured as a function of position [B11]:

$$y = f(x),$$

and the curvature is calculated according to the following formula:

$$R(x) = \frac{\left[1 + (dy/dx)^2\right]^{\frac{3}{2}}}{d^2y/dx^2}.$$

The calculations of the stress are then performed by using the Stoney equation for stress in a thin-film layer deposited on a substrate:

$$\sigma = \frac{1}{6R}\frac{E}{(1-\upsilon)}\frac{t_s^2}{t_f},$$

where σ = stress, t_s = wafer thickness, t_f = film thickness, R = radius of curvature, E = Young's Modulus for the wafer (substrate), and ν = Poisson's Ratio.

5 Experimental set-up, part A: Deposition

The description of the experimental work in this project is divided into two sections, deposition and analysis. The analysis is presented in section 6, while this section is devoted to information regarding the deposition of the silicon nitride films. It begins with the furnace used (section 5.1), and continues with information about processing parameters (section 5.2).

5.1 The LPCVD furnace

In this project a Centrotherm LPCVD horizontal furnace (MC2 tool No. 708), see Figure 5.1, was used to deposit silicon nitride onto silicon wafers. This furnace uses dichlorosilane (DCS) and ammonia (NH_3) as sources for the silicon and nitrogen.

Figure 5.1: The Centrotherm LPCVD horizontal furnace.

Several runs were performed to check the influence of different deposition parameters such as temperature and pressure on the surface topography and stress. For this reason a recipe for the furnace was created, which in each run asked for values of the parameters of interest. The values used here are given in a matrix in section 5.2.

The wafers were 150 mm in diameter and consisted of [100] silicon. Prior to deposition, all wafers were cleaned in SC-1 (RCA-1) and SC-2 (RCA-2) solutions, i.e. standard clean 1 and 2. SC-1 is a mixture of H_2O_2, NH_4OH, and H_2O. In this case, a ratio of 1:1:5 was used (10 minutes, 80 °C). After this process a QDR (quick dump rinser) with H_2O was used, followed by HF etching (2% HF in H_2O, 30 seconds) and again the QDR. SC-2 is a mixture of H_2O_2, HCl, and H_2O. Here, a ratio of 1:1:5 was used (10 minutes, 80 °C). This was again followed by QDR, after which the wafers finally were put in a R&D (rinse and dryer), which uses H_2O and heated N_2 to first rinse and then dry the wafers.

Also, before the deposition process, pre-stress measurements were conducted on the wafers since this is a necessity for the later determination of stress in the silicon nitride layer (see section 4.4).

The wafers were then placed in a quartz boat in the furnace according to the following system:
In each run three marked wafers were used. One was placed near the pump side of the boat, one near the door side, and one in the middle. To simulate a fully loaded boat, these wafers were surrounded by “dummy” wafers, two on each side of the marked wafers, to a total of 15 wafers in each run. Between each run, only the marked wafers were replaced and the other remained at their positions. The side referred to in the text as “the front side of the wafer” was the side facing the door, i.e. facing the gas flow direction.
The boat is shown in Figure 5.2, together with some wafers. It is placed on the loading paddle.

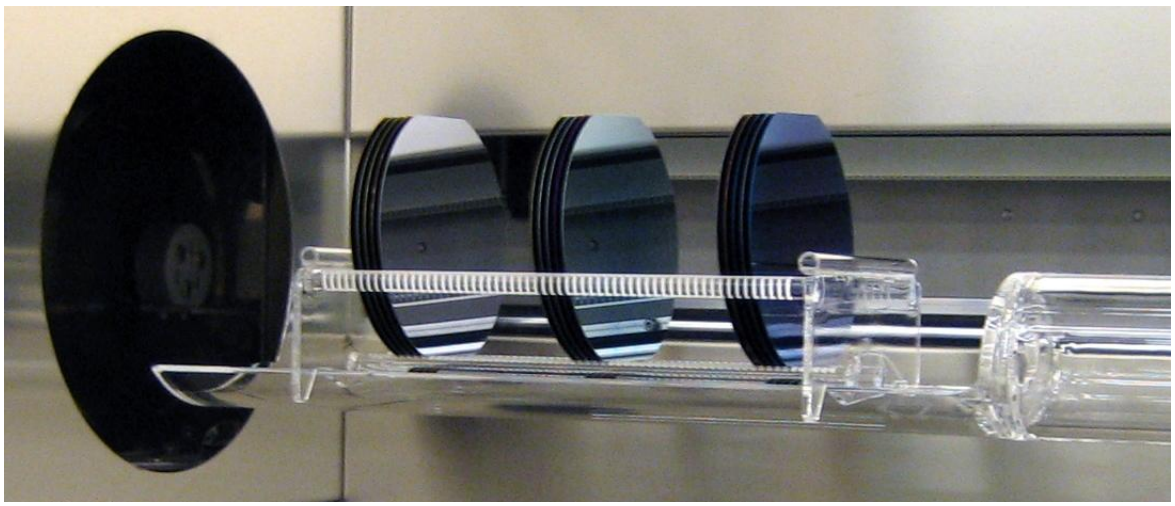

Figure 5.2: The quartz boat used in the LPCVD furnace.

To get a comparable result of the wafers from different runs, a goal of obtaining a silicon nitride layer thickness of approximately 200 nm was set. This was a bit difficult to obtain, in most runs, because of the lack of knowledge regarding the effect of different parameters on the growth rate. Because of this difficulty to determine the deposition time in beforehand, measurements later revealed varying layer thicknesses from between approximately 100 nm to 200 nm. This should not affect the comparability of the different runs.

5.2 Experimental matrix

Since the goal of this project was to investigate how different parameters regarding the furnace affect the properties of the deposited silicon nitride, there was a need for an experimental matrix with values for the parameters during each run. The parameters in question are DCS to NH_3 ratio, total flow (which together with the ratio gives the individual flows), pressure, and temperature. Because of the desired properties of low stress and low surface roughness, the matrix was constructed in a way as to try to meet these requirements. A first estimation on the interesting range for each parameter was obtained through a review of previous work on silicon nitride depositions done by my supervisor. The matrix is also based on information regarding the furnace in question and its limitations, and issues like particle generation had to be considered. An important limitation with this furnace is that the deposition temperature should not be raised above 830 ºC, since this is risky for the vacuum seals.

To get further information on the subject, articles regarding similar projects were consulted [P3] [P4] [P5] [P6]. For example, results from these articles suggested a fairly high DCS:NH_3 ratio to lower the stress. But it was more difficult to find information regarding roughness in published papers, hence the uncertainty in knowing how to apply parameters for low roughness. Also, not all runs were expected to give an optimal result, i.e. lowest stress and lowest roughness. Instead these runs were important for examining the influence of different parameters to get a more general indication of how they affect the outcome.

Altogether, the matrix consisted of twelve different runs, covering the interesting parameter intervals. See Figure 5.3. The temperature range is between 770 °C and 830 °C, the pressure is varied between 150 mTorr and 300 mTorr, the ratio between DCS and NH_3 is placed in the interval of 1:6 up to 6:1, and the total flow lies between 160 sccm (standard cubic centimetres per minute) and 420 sccm.

run number	T (°C)	p (mTorr)	DCS:NH_3 ratio	DCS (sccm)	NH_3 (sccm)	total flow (sccm)
1	770	250	1:6	60	360	420
2	770	250	1:6	50	300	350
3	770	250	1:6	23	137	160
4	770	250	1:3	40	120	160
5	770	250	1:1	80	80	160
6	770	250	4:1	128	32	160
7	820	250	2:1	107	53	160
8	820	250	4:1	128	32	160
9	820	250	6:1	137	23	160
10	820	150	4:1	128	32	160
11	820	300	4:1	128	32	160
12	830	250	4:1	128	32	160

Figure 5.3: The experimental matrix.

6 Experimental set-up, part B: Analysis

Several different techniques were used in analysing the deposited silicon nitride layer. Firstly, the thickness of the layer, together with the refractive index, was determined using ellipsometry. Together with the deposition time for the wafer in question, this allowed the deposition rate to be calculated, simply by dividing thickness with deposition time. Secondly, scanning probe microscopy (SPM) in the form of atomic force microscopy (AFM) provided roughness measurements of the surface. Thirdly, plasma etching was used to remove the silicon nitride deposited on the back of the wafers, enabling stress measurements to be made on the layer deposited on the front side of the wafer. Finally, these stress measurements were performed with a profilometer. The following subsections provide a fuller description of how these techniques were used in this project, and the results are presented in section 7.

6.1 Thickness measurements

The ellipsometry measurements were performed with a J.A. Woollam M2000 spectroscopic ellipsometer (MC2 tool No. 112), using the software WVASE (Variable Angle Spectroscopic Ellipsometry for Windows). This equipment is shown in Figure 6.1. With this ellipsometer, the ellipsometric angles are given as functions of wavelength.

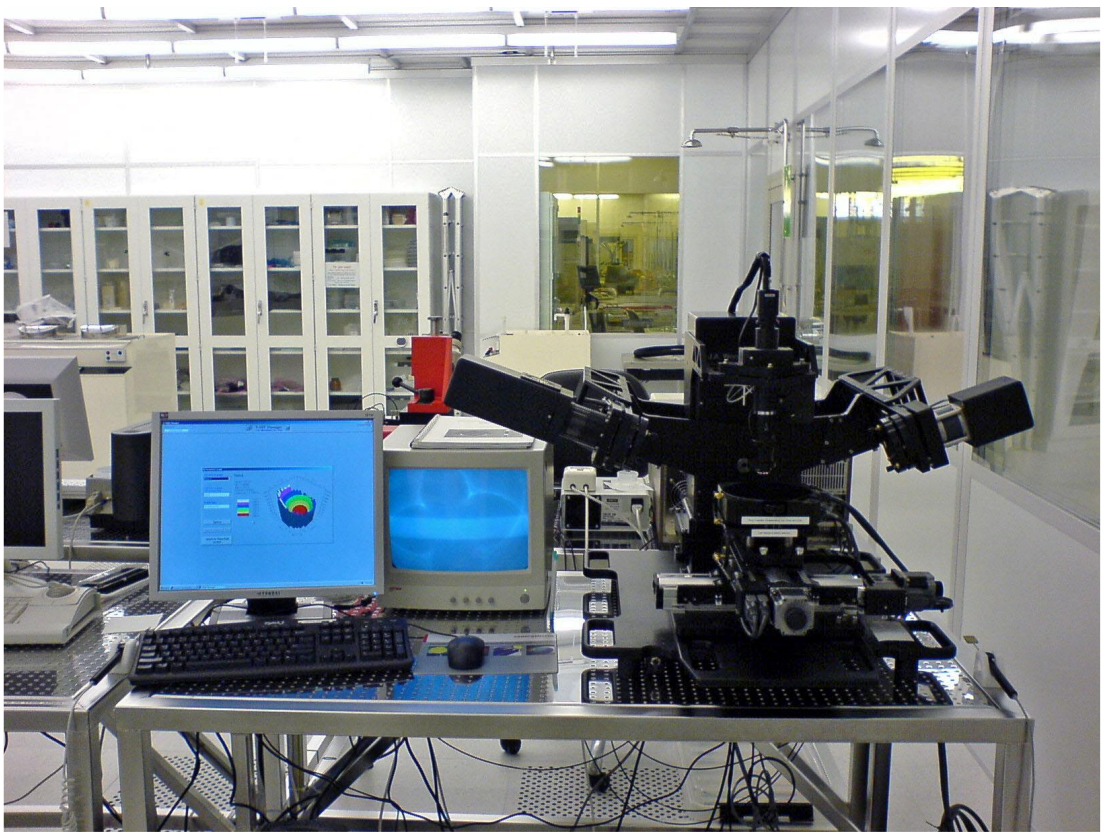

Figure 6.1: The J.A. Woollam M2000 spectroscopic ellipsometer.

Measurements were made in the middle of each wafer at an angle of 70 degrees, and models were built. Depending on differences in film compositions between the different runs, not all wafers could be analysed with the same model. Instead different layer compositions in the model had to be constructed in order to obtain a fit with a reasonable low mean square error (MSE, Section 4.1). The calculations of the thickness, together with the deposition time, gave the deposition rates, simply by dividing thickness with time. Also, refractive index (n) at the wavelength (λ) of 632.8 nm was extracted from the n(λ) data set.

Besides this value of thickness in the middle of the wafers, it is also of interest to see the variations in thickness over the entire surface of a wafer, i.e. the uniformity over the wafer. Therefore, a pattern of 69 points of measurement was established in order to sufficiently cover the entire surface. (The pattern had a diameter of 13 cm, excluding the parts near the edge of the wafer.) For this part, another software from Woollam called VASEM (where M stands for Manager) was used. This software automatically moves the point of measurement according to the given pattern and also matches every point to a given model. Again, an angle of 70 degrees was used. There are suggestions that three-angle measurements would give a more correct value. This was tested through a three-angle measurement using 65, 70 and 75 degrees, on two of the wafers. The results differed with about one nanometre, or less, from the results obtained with one-angle measurements using 70 degrees, for both of the wafers. Since the thicknesses of the films were between 100 nm to 200 nm, the 1 nm measurement difference represents one percent or less of the true total thickness, i.e. a negligible difference. Therefore, one-angle measurements were used throughout all measurements.

The pattern measurements were only used on the wafer in the middle of the boat, since a similar outcome was expected for the left- and right-hand wafers. The variations in thickness were calculated based on the maximum and minimum values of the thickness according to the formula:

$$\frac{\max - \min}{\max + \min}.$$

Based on these results it was possible to establish which wafer had the least variation in thickness and which had the greatest variation. These two wafers were again analysed using a pattern of 177 points in VASEM. Two graphs based on the results were then obtained through interpolation between these points by the software.

Also, the average thickness was calculated according to:

$$\frac{\max + \min}{2}.$$

These values were later used in stress calculations (see section 6.3).

6.2 Roughness measurements

The SPM measurements were performed with a Digital Instrument Dimension 3000 SPM (MC2 tool No. 111), which is displayed in Figure 6.2.

Figure 6.2: The Digital Instrument Dimension 3000 SPM used for roughness measurements.

Because of similarity between surfaces from the same run but with different placing in the boat, measurements were only performed on the wafer placed in the middle of the boat. Each surface was scanned three times at different points from the edge to near the middle of the wafer. By taking a mean value of the obtained roughness in these three points, the accuracy of the measurement increased since the risk of getting an incorrect value caused by random artefacts was minimised. The scan sizes were 1x0.5 μm for some wafers, and 1x1 μm for wafers where a higher scan speed could be applied. PSD was calculated for the scan taken between the edge of the wafer and the middle point (no significant difference was shown when compared for instance with PSD calculations of the scan near the edge of the wafer).

6.3 Stress measurements

Before stress measurements could be made, the deposited silicon nitride had to be removed from the backside of the wafers, since the stress in the layers on opposite sides of the wafer otherwise would cancel each other out. Plasma etching was used to remove the layer from the back of the wafer placed in the middle of the boat. This was done with a Plasma Therm Batchtop PE/RIE m/95 (MC2 tool No. 419), using freon (CF_4) gas. This equipment is shown in Figure 6.3.

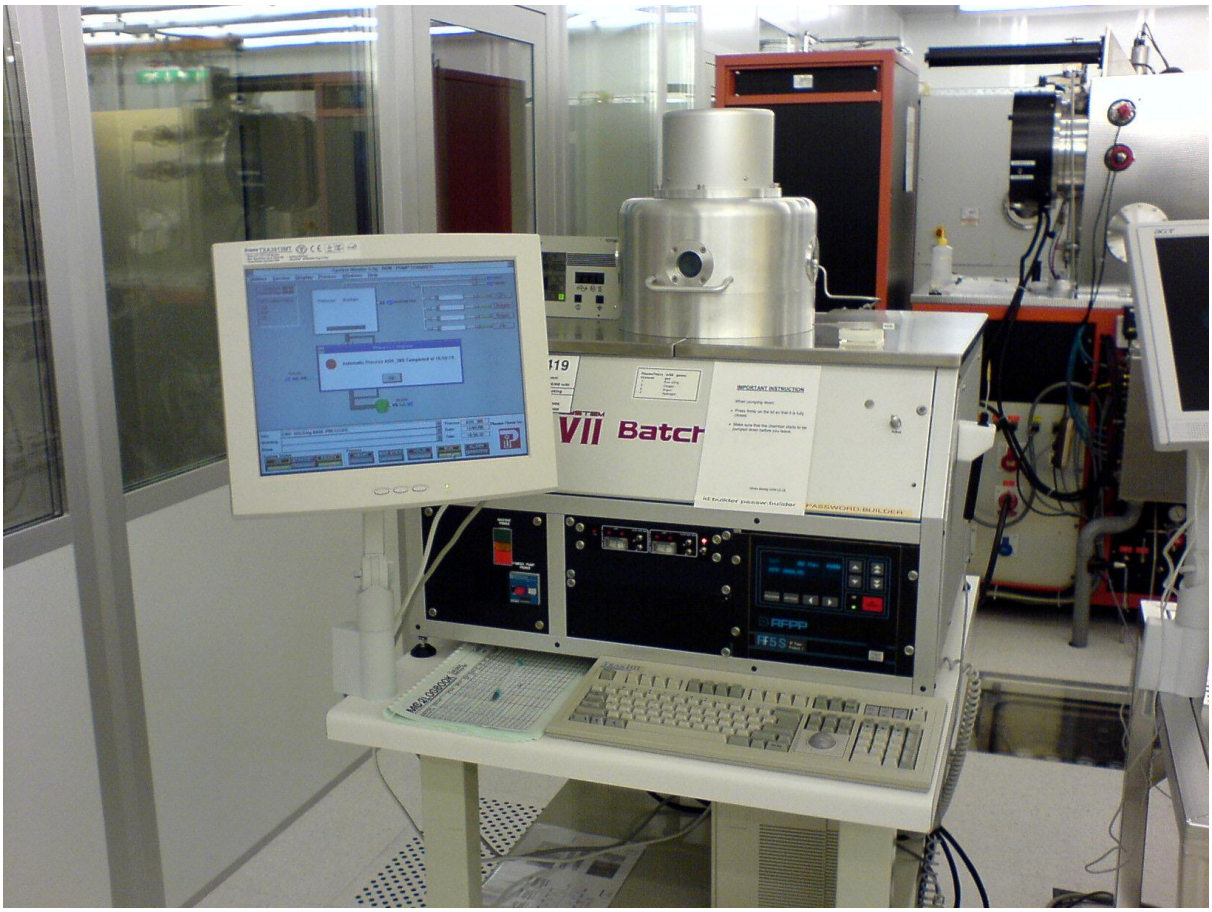

Figure 6.3: The Plasma Therm Batchtop PE/RIE m/95 used for etching.

Stress measurements were made with a Tencor P15 stylus surface profiler (MC2 tool No. 108). This equipment is displayed in Figure 6.4.

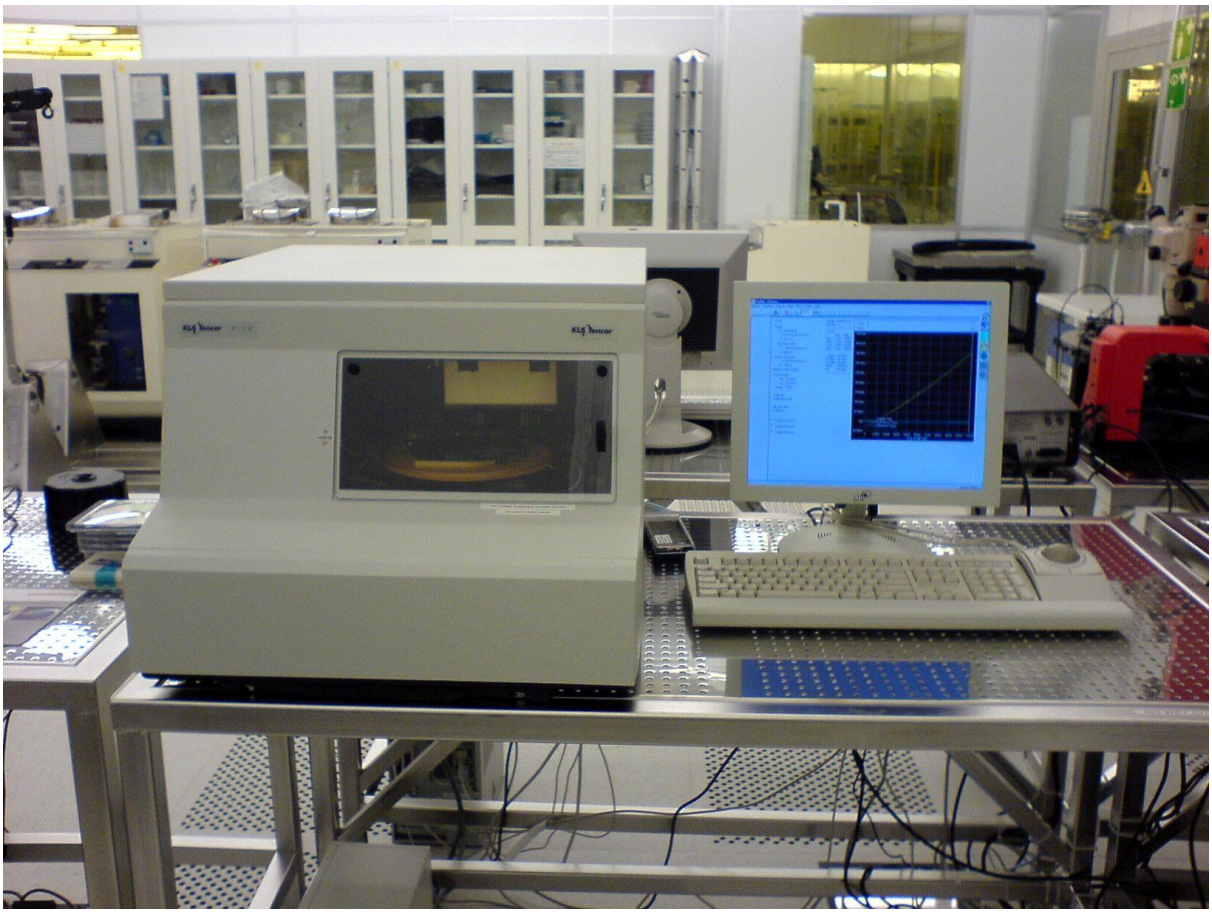

Figure 6.4: The stylus surface profiler Tencor P15 used for stress measurements.

Since the silicon nitride on the backside of the wafers had been removed each of the middle wafers now only had silicon nitride deposited on the front side. Therefore, a stress scan of this surface could be made, and by comparison with the scan of the same surface made prior to deposition (see section 5.1), the stress in the deposited layer could be determined. This was made automatically by the profiler software through calculations based on the pre- and post-scans together with the thickness of the deposited layer (previously determined by ellipsometry, section 6.1).
The length of the scan was 12 cm, and it was performed through the centre point of the wafer.

7 Results and evaluations

For an easier view of the results from the previous experimental descriptions, the matrix from section 5.2 is displayed again in Figure 7.1.

run number	T (°C)	p (mTorr)	DCS:NH_3 ratio	DCS (sccm)	NH_3 (sccm)	total flow (sccm)
1	770	250	1:6	60	360	420
2	770	250	1:6	50	300	350
3	770	250	1:6	23	137	160
4	770	250	1:3	40	120	160
5	770	250	1:1	80	80	160
6	770	250	4:1	128	32	160
7	820	250	2:1	107	53	160
8	820	250	4:1	128	32	160
9	820	250	6:1	137	23	160
10	820	150	4:1	128	32	160
11	820	300	4:1	128	32	160
12	830	250	4:1	128	32	160

Figure 7.1: The experimental matrix from section 5.2.

In the following subsections, measurements from the different analysis methods are given in graphical form. They show the obtained refractive index, section 7.1, deposition rate, section 7.2, thickness uniformity, section 7.3, roughness, section 7.4, and stress, section 7.5. To enhance the readability of these graphs, runs with different temperatures have been given different colours. Also, some other additional graphs are given in every subsection to highlight the main statements made in each evaluation. This will hopefully help to clarify the main graph without the need to look back into the matrix in detail.

7.1 Refractive index

Results from measurements of refractive index are given in Figure 7.2. Each measurement was performed on the middle of the wafer and the values were obtained at a wavelength of 632.8 nm. Displayed values are average refractive index based on all three wafers in each run (values between wafers in the same run did not differ significantly, only in the second decimal in some cases).

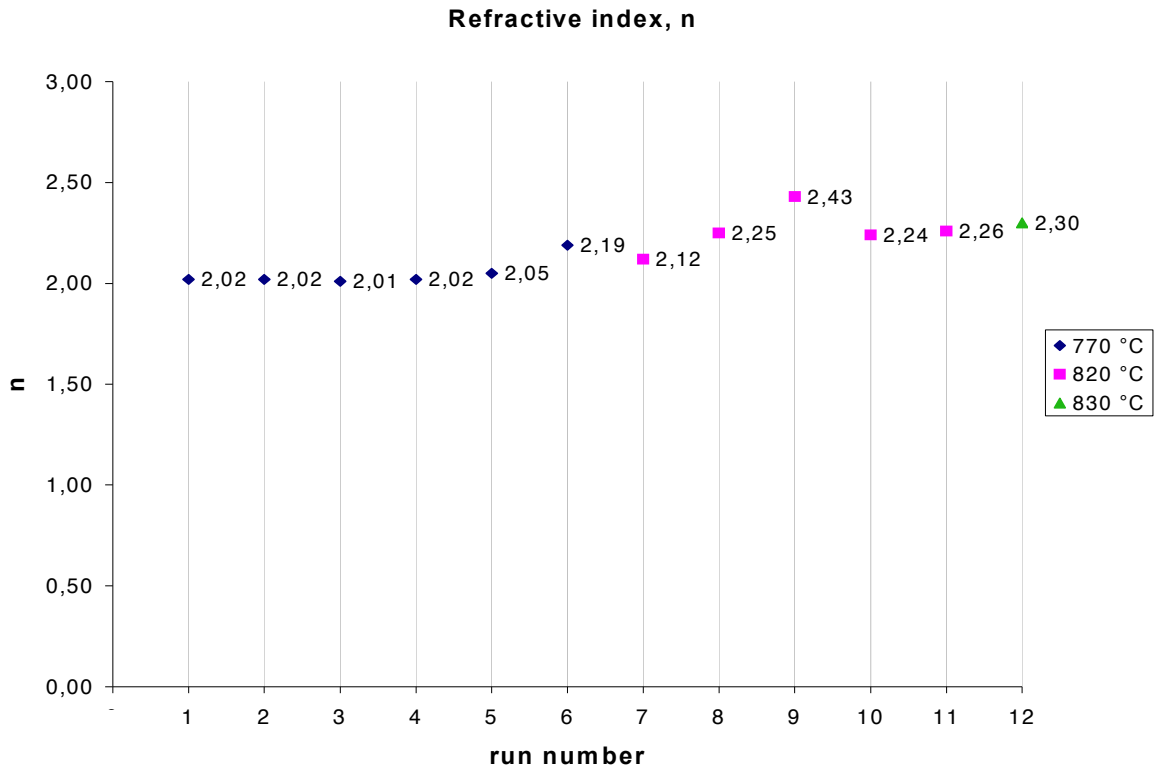

Figure 7.2: Results from measurements of refractive index.

The data presented in Figure 7.2 clearly shows that increasing the DCS:NH_3 ratio gives a higher refractive index. A ratio of 6:1 gave a refractive index as high as 2.43, far from the ideal value of 2.0. Also, a very slight increase in refractive index because of temperature can be seen. The relation between refractive index and gas ratio is shown in Figure 7.3a, and the relation between refractive index and temperature is displayed in Figure 7.3b.

Changes in pressure or total flow did not show any influence on refractive index.

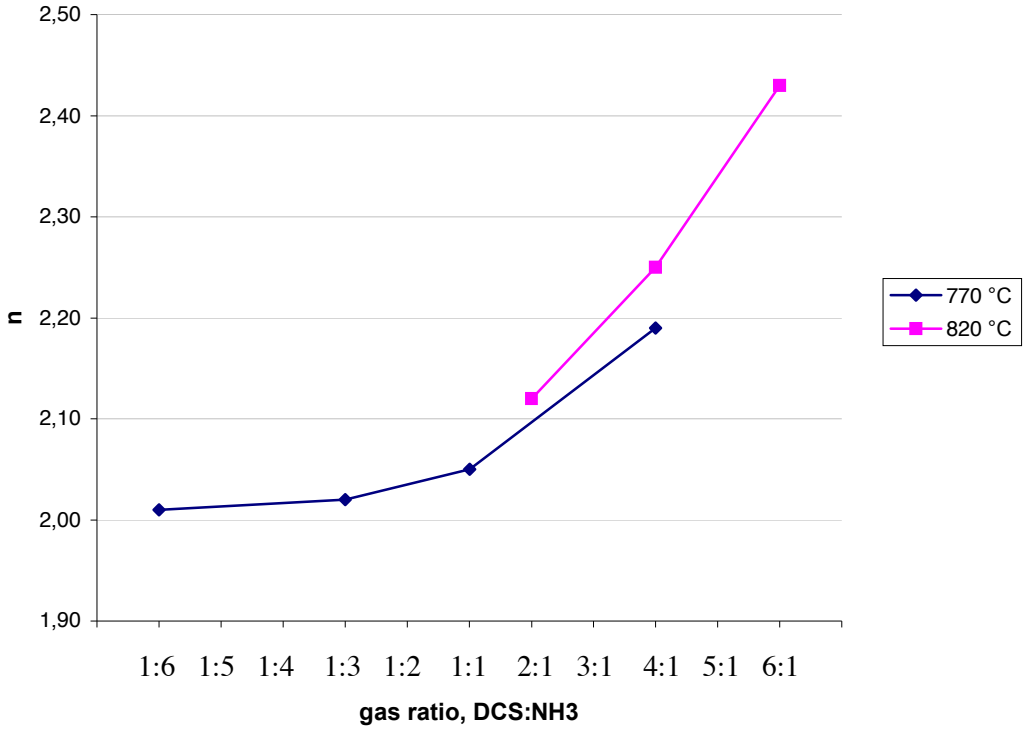

Figure 7.3a): (Above) Relation between refractive index and gas ratio, at two different temperatures.

b): (Right) Relation between refractive index and temperature.

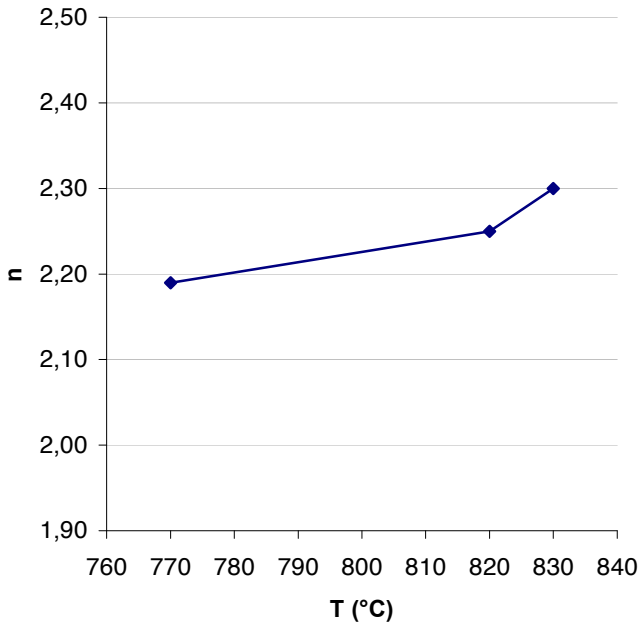

7.2 Deposition rate

Results from calculations of deposition rates are shown in Figure 7.4. Each measurement was performed on the middle of the wafer. Displayed values are average deposition rate based on all three wafers in each run.

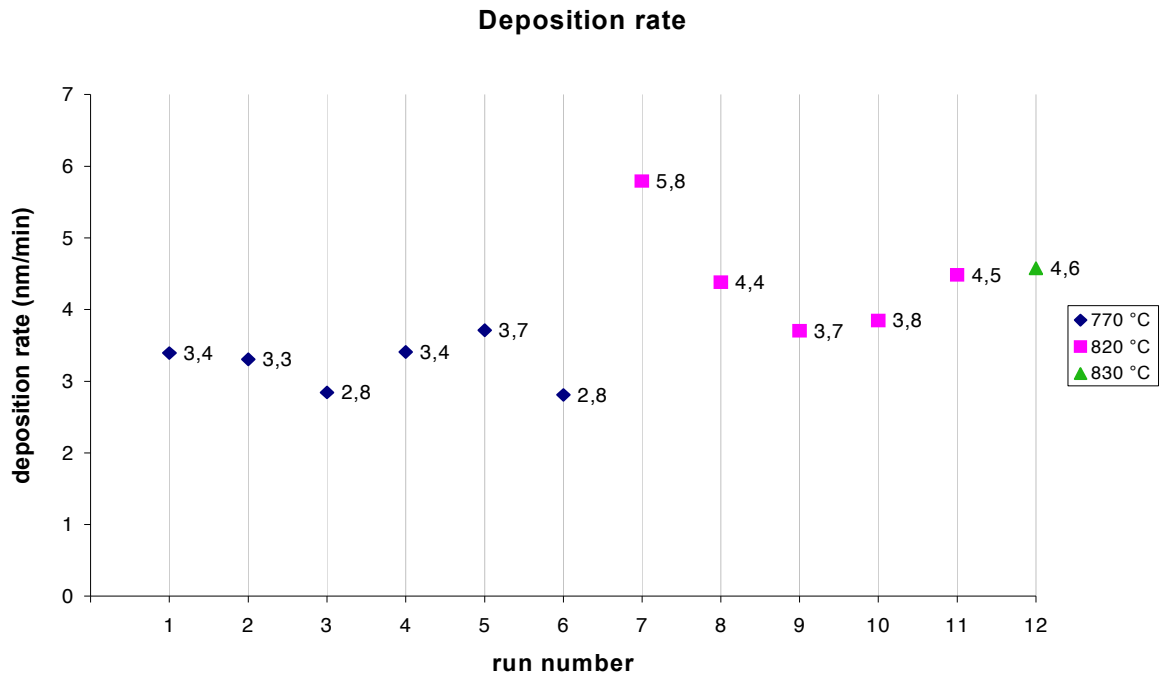

Figure 7.4: Results from calculations of deposition rates.

The data presented in Figure 7.4 shows a decreasing deposition rate with decreasing total flow. Also, an increase of deposition rate with increasing temperature can be seen. The low deposition rate in run number 6 and the high value in run number 7, decreasing through 8 and 9, indicate an influence of DCS:NH_3 ratio. Pressure also seems to have a slight influence, since increasing the pressure also increases the deposition rate. All of these relations are shown in Figure 7.5.

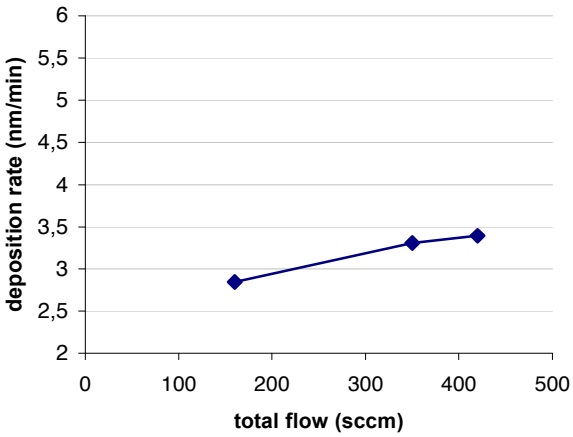

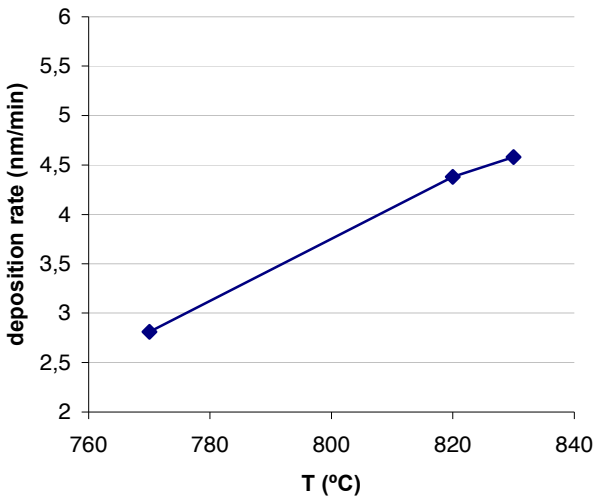

Figure 7.5a): (Above, left) Relation between deposition rate and total flow.

b): (Above, right) Relation between deposition rate and temperature.

c): (Right) Relation between deposition rate and pressure.

d): (Below) Relation between deposition rate and gas ratio, at two different temperatures. Equal flows of DCS and NH_3 give the highest deposition rate.

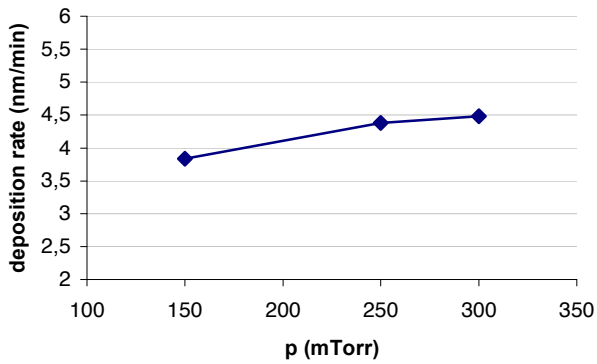

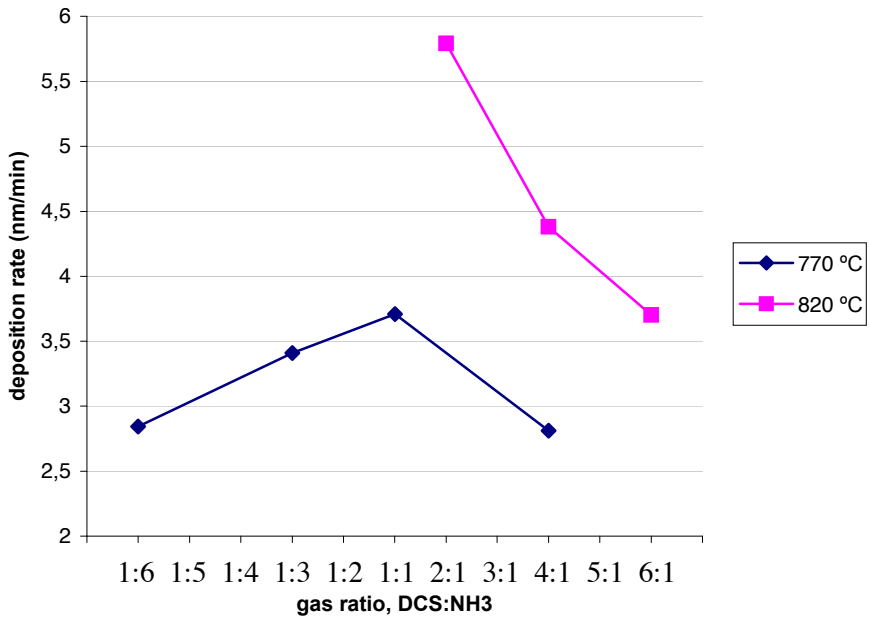

7.3 Thickness uniformity

Results from calculations of thickness uniformity are shown in Figure 7.6. Displayed values are variations in thickness over a single wafer, for the middle wafer in each run.

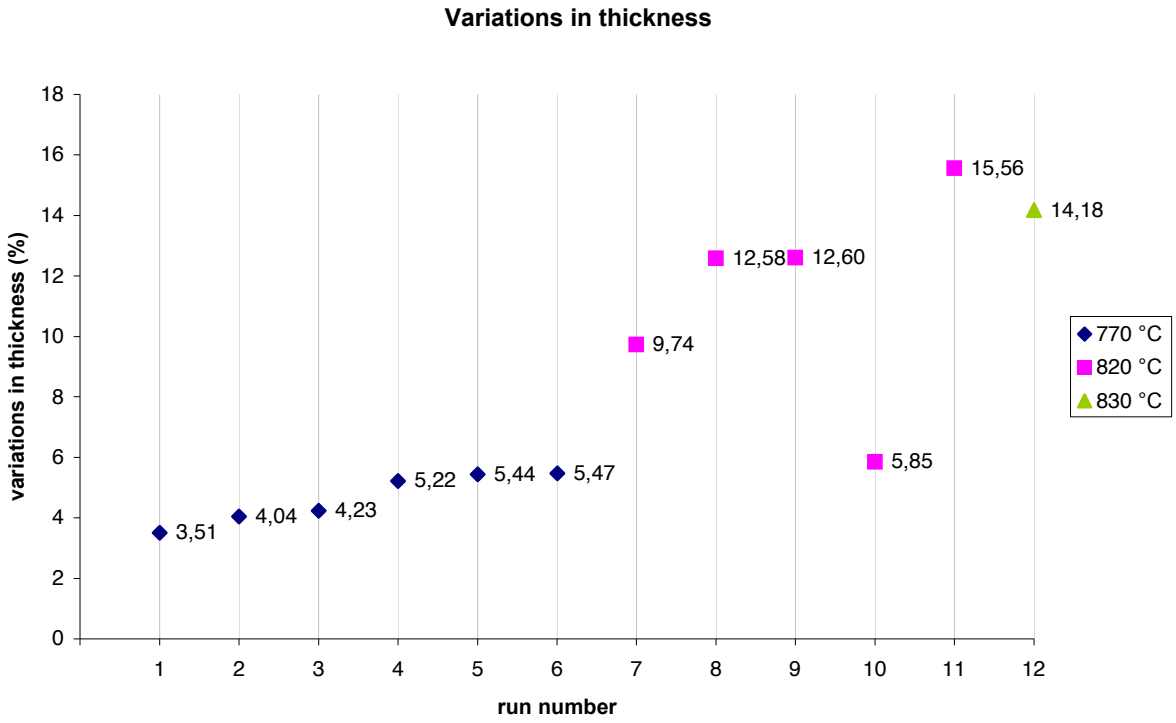

Figure 7.6: Results from calculations of variations in thickness over a single wafer.

The data presented in Figure 7.6 shows decreasing uniformity with increasing temperature and to a lesser extent DCS:NH_3 ratio. Also, pressure is seen to be very important for variation in thickness, with an increasing variation in thickness with increasing pressure. Total flow does not have any significant influence. The two most important relations are shown in Figure 7.7. Figure 7.7a shows the dependence of temperature, while Figure 7.7b displays the influence of pressure.

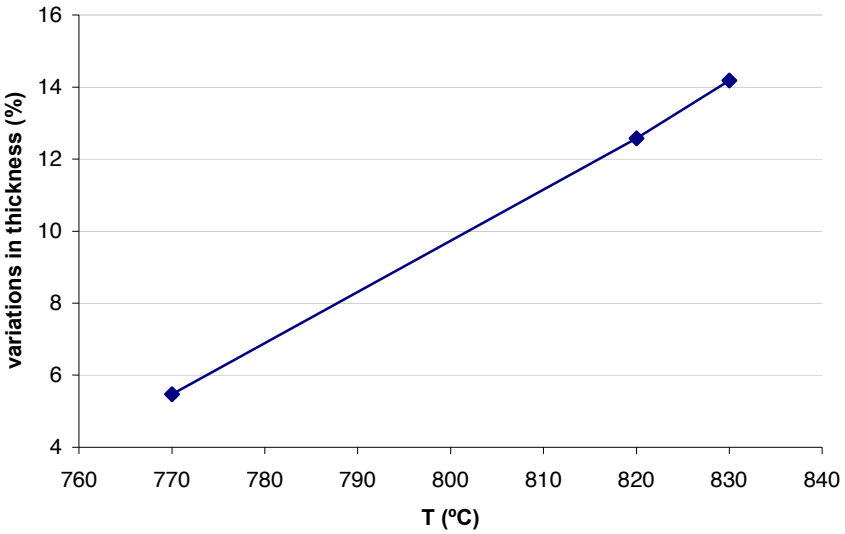

Figure 7.7a): (Above) Relation between variations in thickness and temperature.

b): (Right) Relation between variations in thickness and pressure.

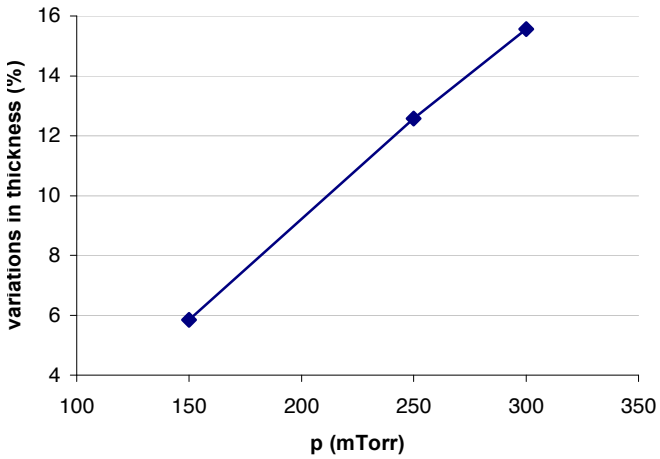

The wafer from run number 1 had the least variation in thickness, and the wafer from run number 11 had the greatest variation. These two wafers were analysed again (see section 6.1) and the result from these new measurements is given in Figure 7.8. Figure 7.8a shows the wafer with least variation, and Figure 7.8b shows the wafer with greatest variation.

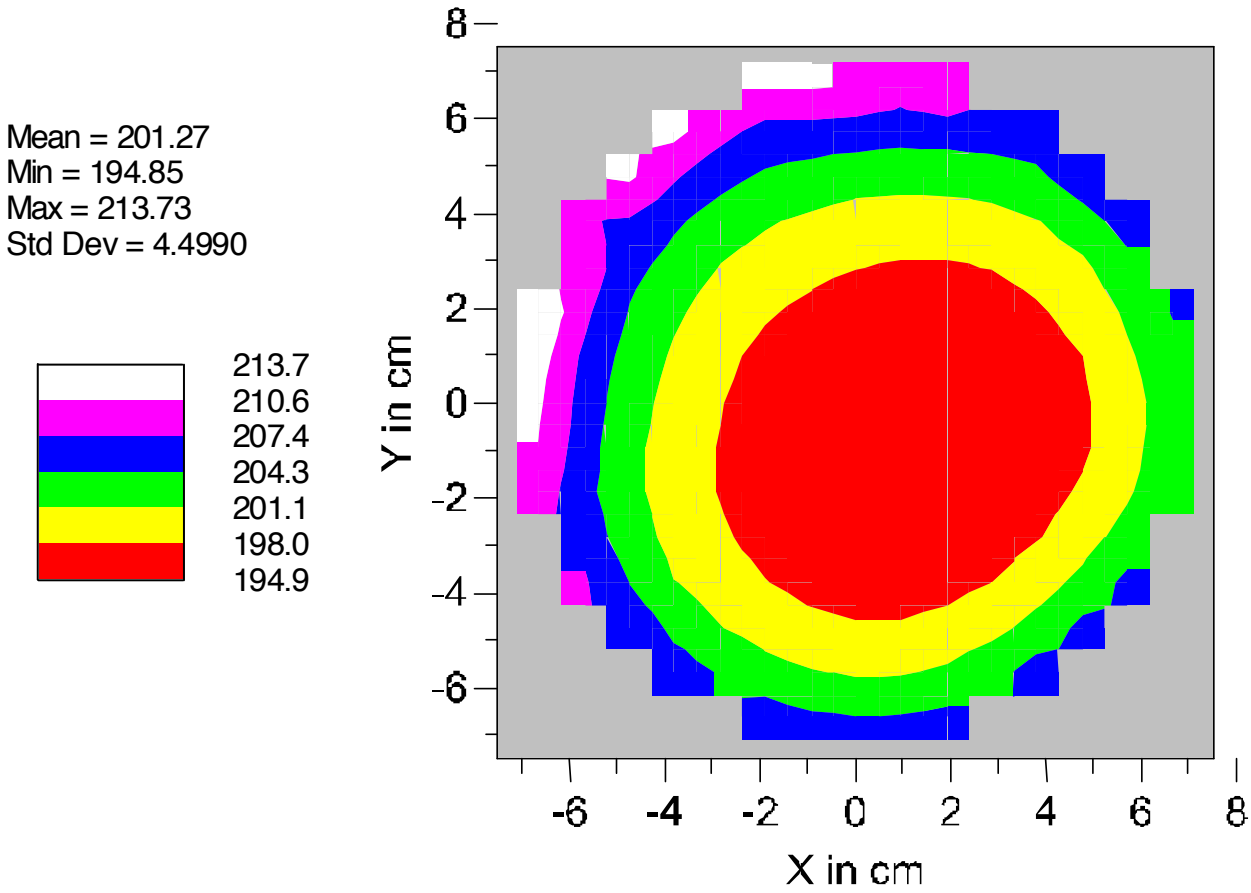

Figure 7.8 a): (Above) Variations in thickness for the deposited thin film with least variations. The thickness varies between 194.9 nm in the middle of the wafer, and 213.7 nm near the edge.
Deposition parameters: T = 770 °C, p = 250 mTorr, DCS:NH_3 ratio = 1:6, total flow = 420 sccm.

b): (Next page) Variations in thickness for the deposited thin film with greatest variations. The thickness varies between 115.6 nm in the middle of the wafer, and 166.3 nm near the edge.
Deposition parameters: T = 820 °C, p = 300 mTorr, DCS:NH_3 ratio = 4:1, total flow = 160 sccm.

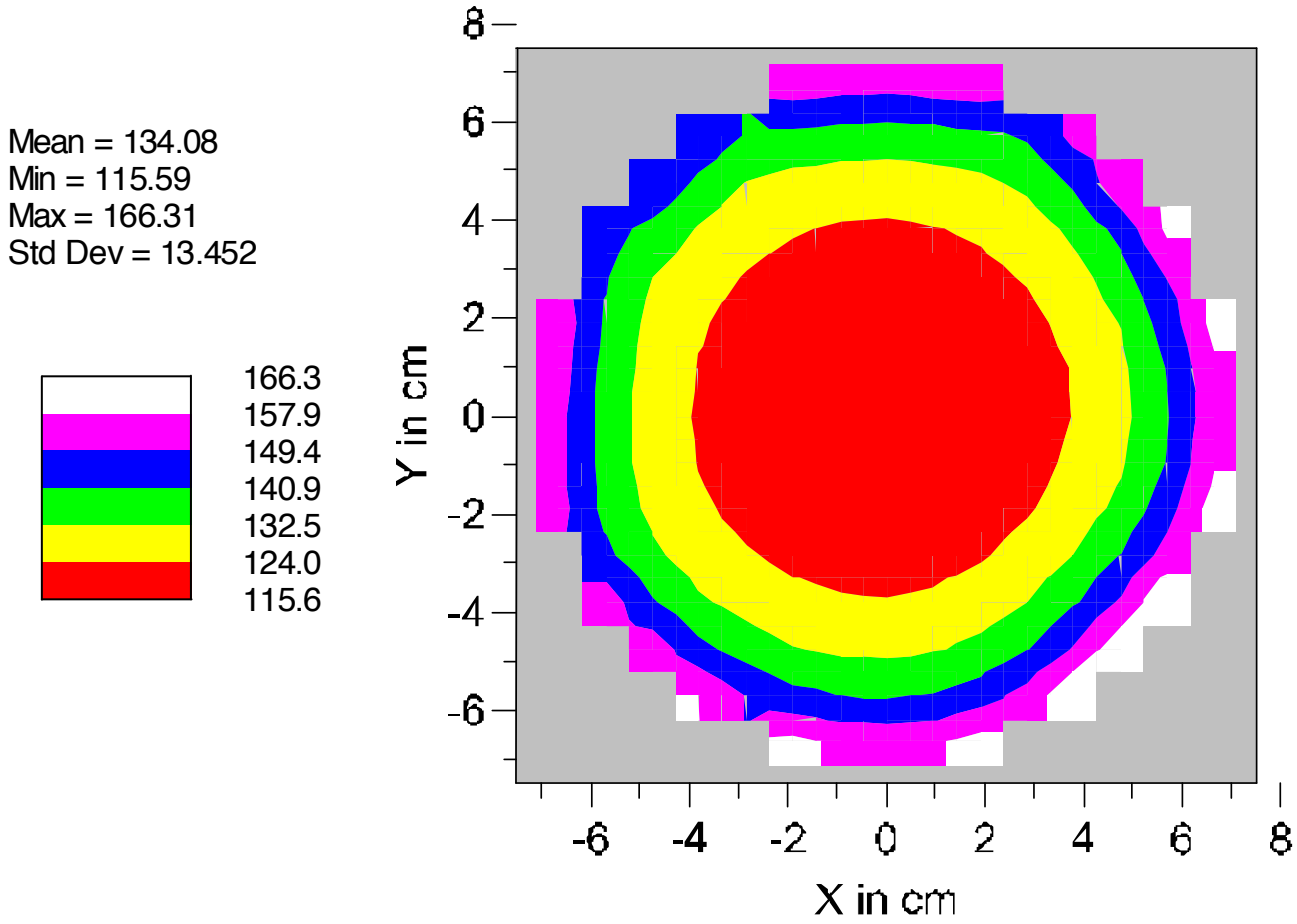

Figure 7.9 shows the average thicknesses needed for stress calculations.

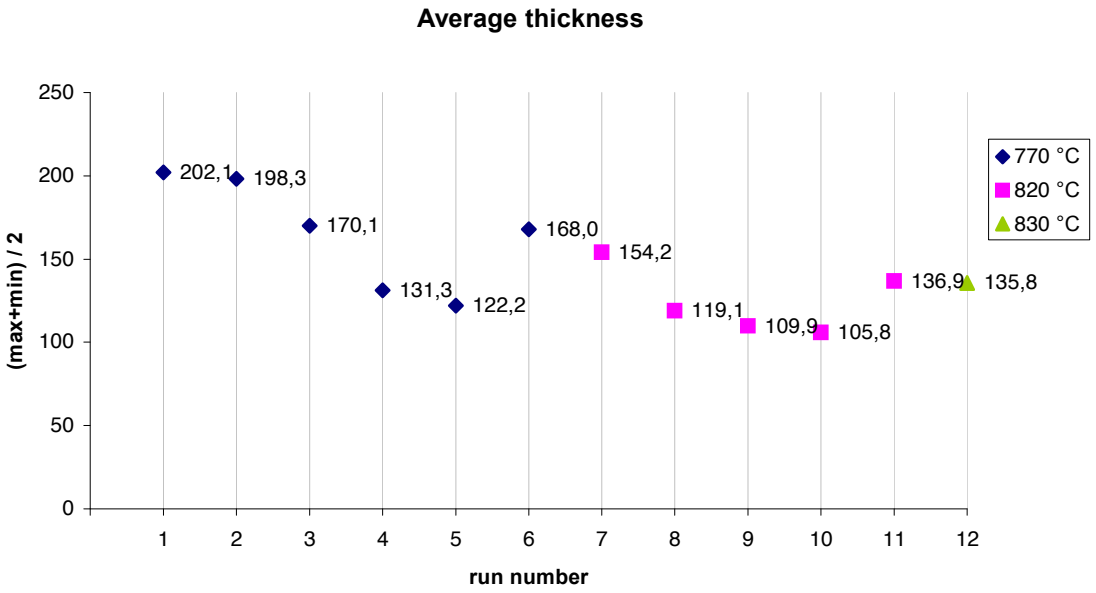

Figure 7.9: Average thicknesses calculated as (maximum thickness + minimum thickness) / 2.

7.4 Roughness

Results from measurements of RMS roughness are shown in Figure 7.10. Displayed values are average RMS roughness based on all three measurements on the wafer placed in the middle of the boat.

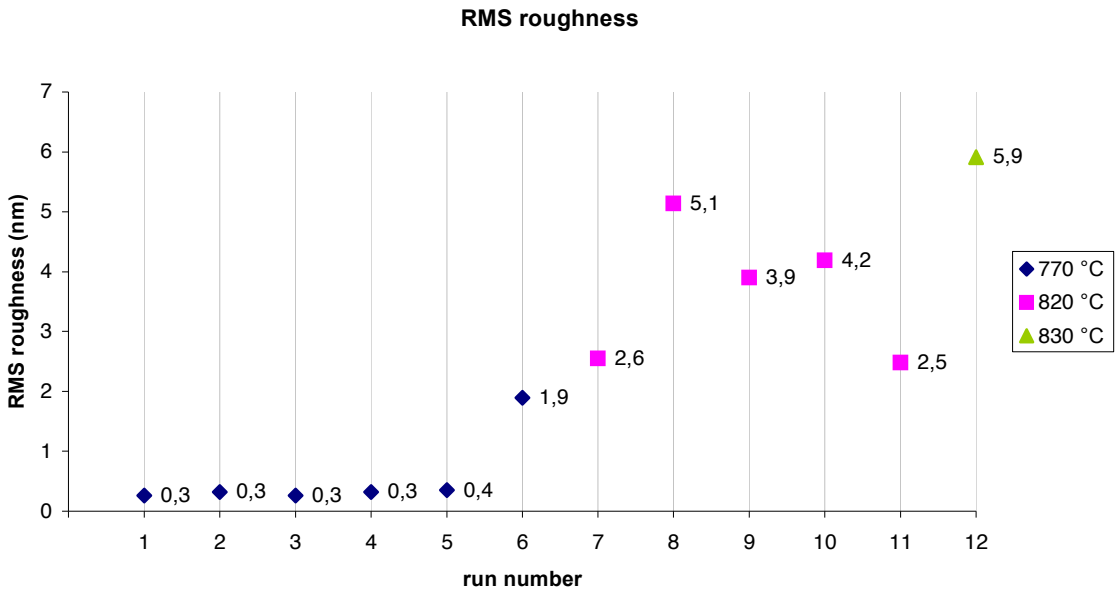

Figure 7.10: Results from measurements of RMS roughness.

The data presented in Figure 7.10 shows an increasing RMS roughness with increasing temperature. Although differing values of the RMS roughness are shown when the pressure and gas ratio are varied, no general conclusions can be stated based on each parameter since they do not have a clear trend towards increasing or decreasing values. For example, a pressure of 300 mTorr gives a RMS value of 2.5 nm, and a pressure of 150 mTorr gives a RMS value of 4.2 nm. For an indication of the relation between pressure and RMS roughness, a pressure of 250 mTorr would be expected to give a RMS value between 2.5 and 4.2 nm, but instead this value became the highest (5.1 nm). Instead, there seems to be some sort of relation between RMS roughness and the combination of pressure and gas ratio. Even so, the RMS values from run number 5 and 6 clearly show that a low gas ratio is preferred for obtaining a low RMS roughness. The total flow did not affect the roughness.

The relation between temperature and RMS roughness is shown in Figure 7.11.

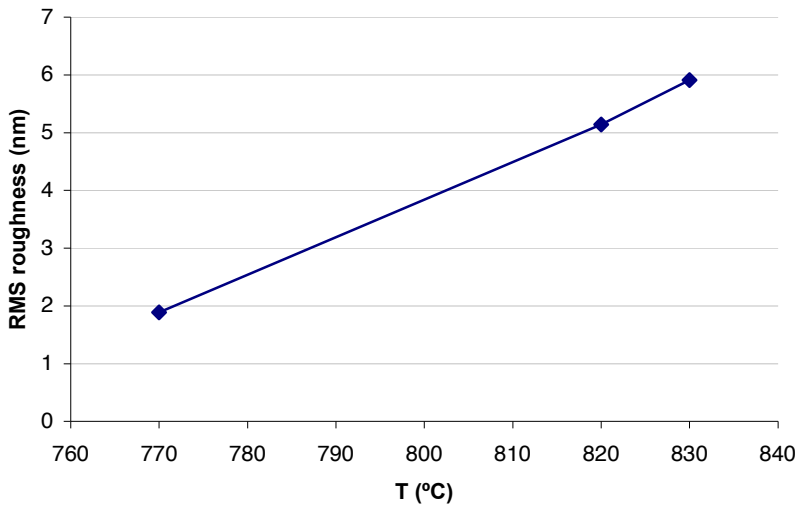

Figure 7.11: Relation between temperature and RMS roughness.

Results from measurements of PSD are shown in Figure 7.12. Because of the very low RMS roughness in the first 5 runs, shown in Figure 7.10, these surfaces are not of much interest for PSD measurements since they cannot have such large spikes that bonding would be prevented. Even so, the PSD curves that differed the most between these first 5 runs are shown in Figure 7.12a, to give an idea of how much they differ from PSD curves from surfaces with higher RMS roughness values. Figure 7.12b shows two PSD curves from surfaces with about the same RMS roughness values, namely from run number 7 and 11. When comparing Figure 7.12a with Figure 7.12b, it is important to note the large difference in PSD scales in the two graphs.

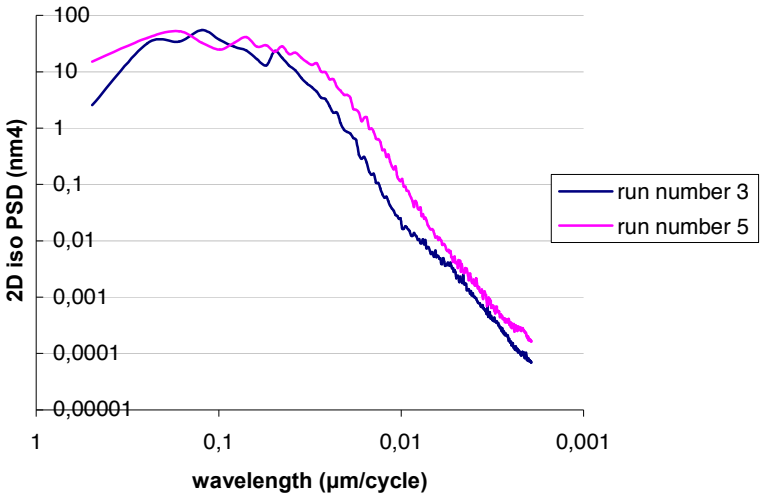

Figure 7.12a): (Above) Two PSD curves from surfaces with low RMS roughness values.

b): (Below) Two PSD curves from surfaces with about the same RMS roughness values.

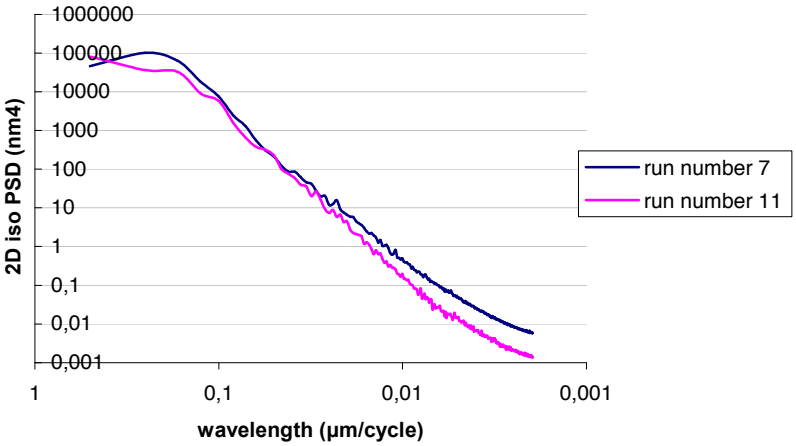

For the whole frequency domain, the wafer from run number 11 shows a decrease in roughness compared with the wafer from run number 7. The curves in Figure 7.12b are also almost parallel, except for the smallest wavelengths, which indicate a similar roughness distribution.

Figure 7.13 shows PSD measurement results for the rest of the wafers that had quite high RMS roughness.

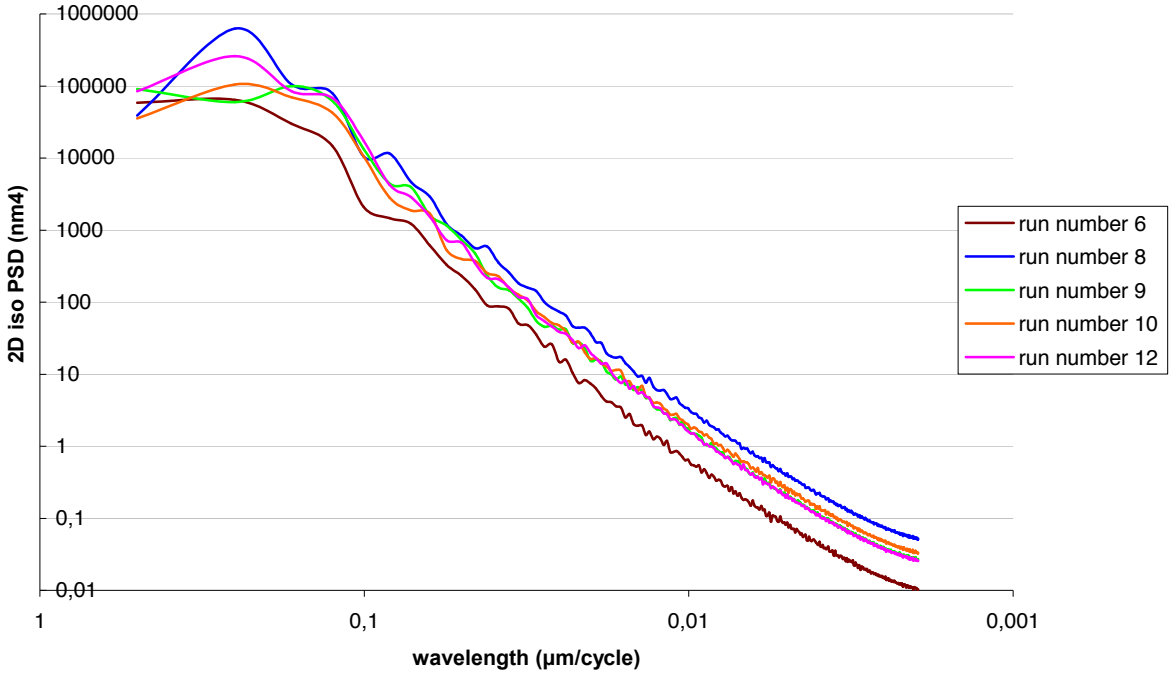

Figure 7.13: PSD for wafers with high RMS roughness values.

The data in Figure 7.13 shows that these wafers, in general, had a similar roughness distribution.

Two of the scans obtained during the AFM measurements are shown in Figure 7.14. Figure 7.14a shows a scan of a surface with very low roughness, taken from run number 2. Figure 7.14b shows a scan of a surface with very high roughness, taken from run number 12. It is important to note the difference in height scales in the two scans. While the first scan has small spikes with a maximum height of approximately 4 nm, the largest spike in the second scan is as high as about 60 nm.

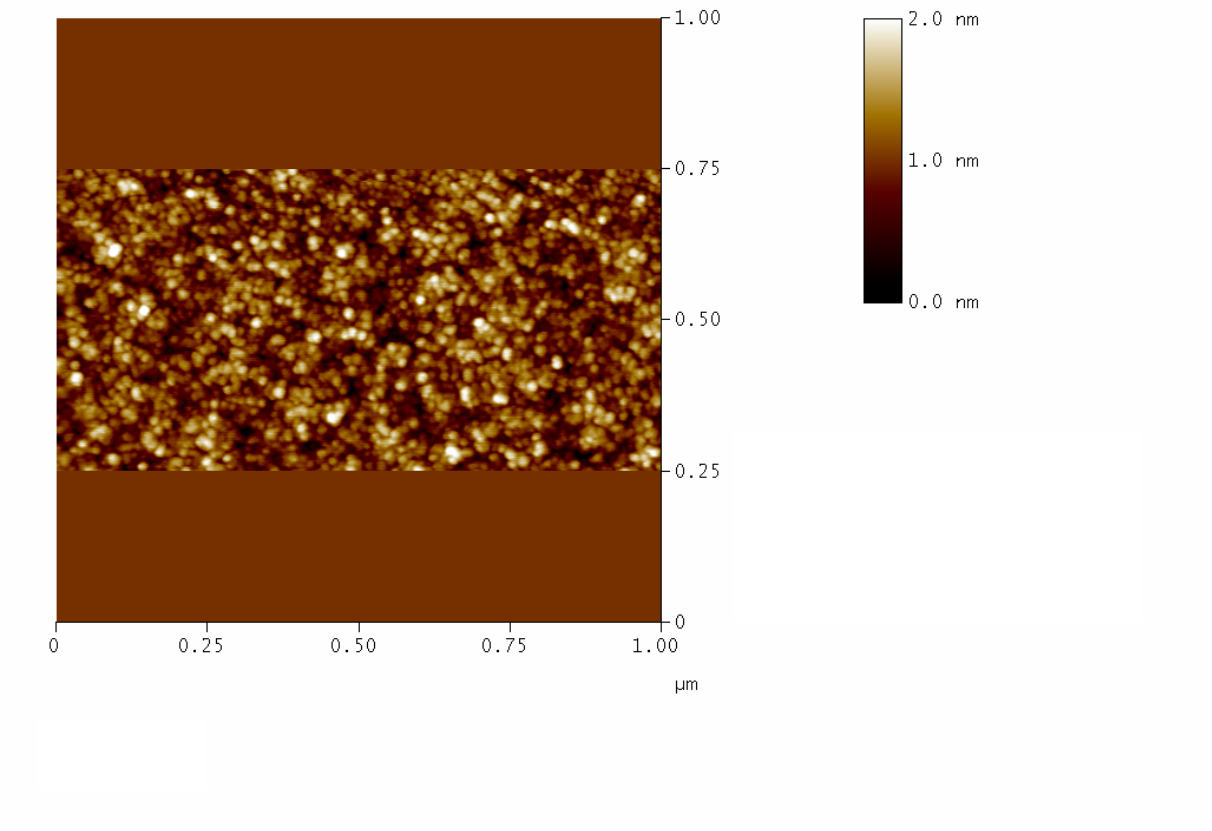

Figure 7.14 a): (Above) AFM scan of a surface with low roughness, height scale up to 2.0 nm. Deposition parameters: T = 770 °C, p = 250 mTorr, DCS:NH_3 ratio = 1:6, total flow = 350 sccm. Scan size: 1.0 x 0.50 µm, hence the uniform colour outside the scan area.

b): (Next page) AFM scan of a surface with high roughness, height scale up to 40.0 nm. Deposition parameters: T = 830 °C, p = 250 mTorr, DCS:NH_3 ratio = 4:1, total flow = 160 sccm.

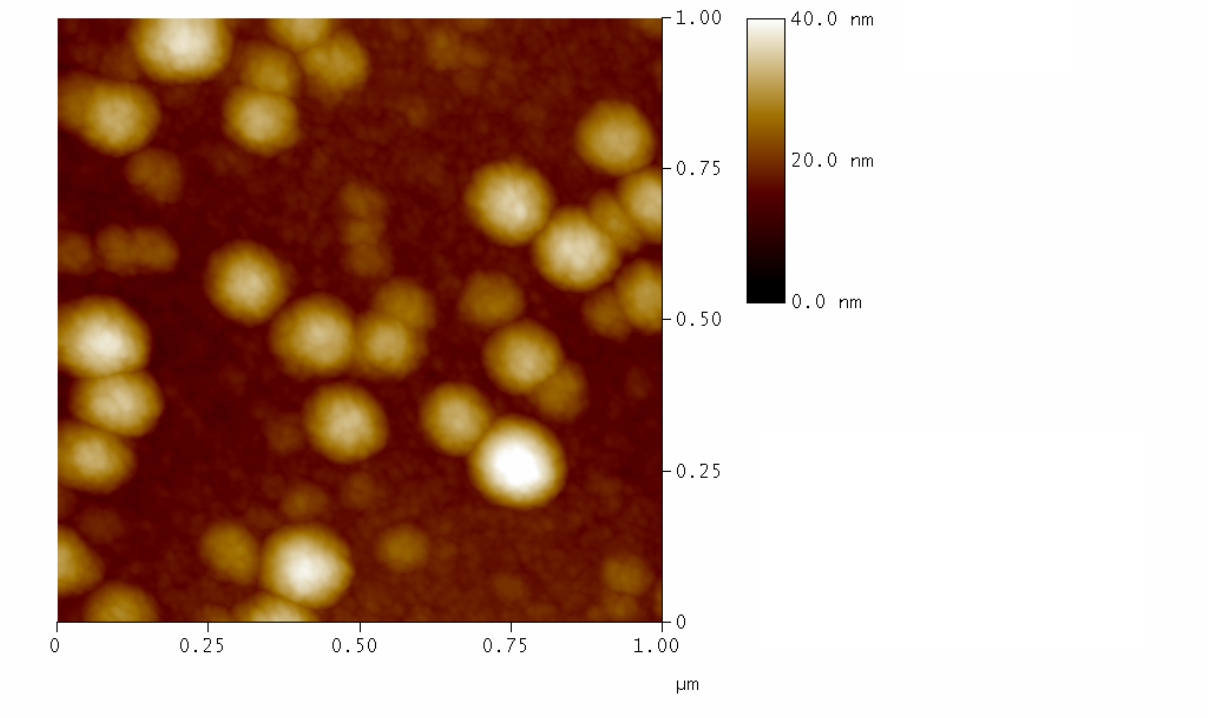

Besides these two extreme cases with very high and very low roughness, it is interesting to take a closer look on a scan of a surface where the roughness has begun to increase from the very low values of the first five runs. The scan in Figure 7.15 is taken from run number 6, and has spikes as high as 30-40 nm.

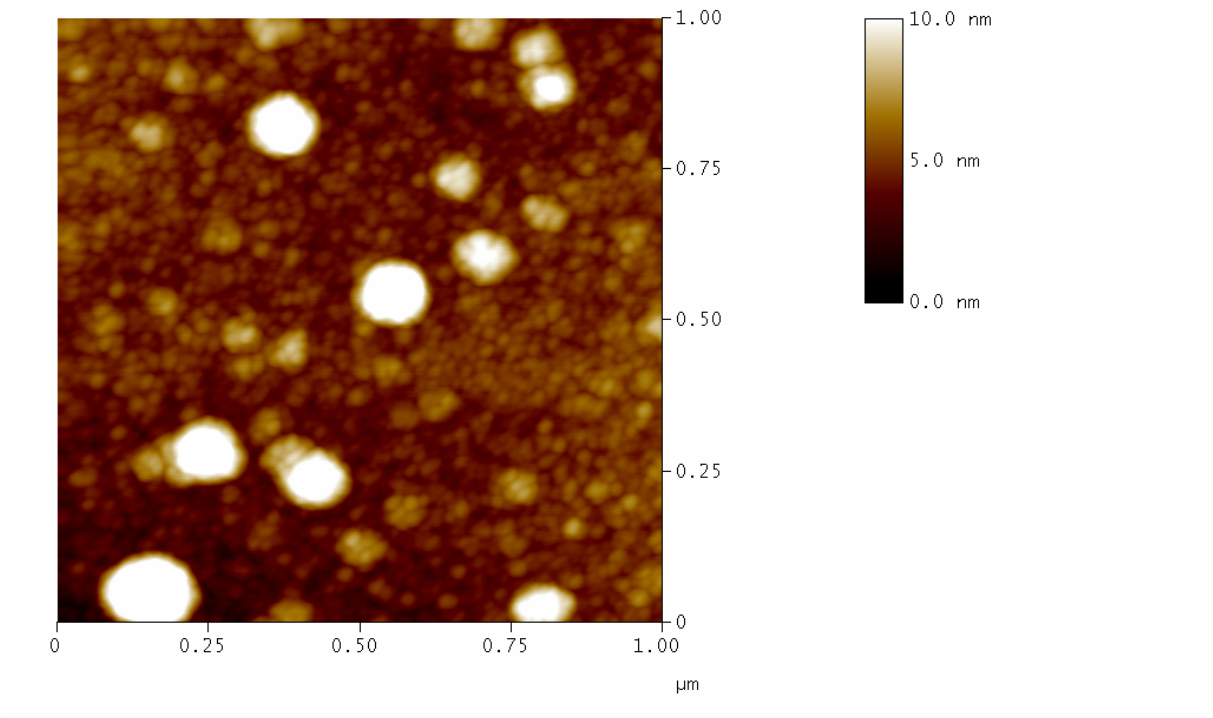

Figure 7.15: AFM scan of a surface with medium roughness, height scale up to 10.0 nm.
Deposition parameters: T = 770 °C, p = 250 mTorr, DCS:NH_3 ratio = 4:1, total flow = 160 sccm.

7.5 Stress

Results from stress measurements are shown in Figure 7.16. Measurements were performed on the wafer placed in the middle from each run. Displayed values are the average value over the entire profile on each wafer and they are given together with the maximum absolute stress.

Figure 7.16: Results from stress measurements.

The data presented in Figure 7.16 shows a decreasing tensile stress with increasing DCS:NH_3 ratio. The stress even becomes slightly compressive for the highest ratio of 6:1. The stress is also decreasing with higher temperature. A slight decrease with decreasing pressure is also seen. Lowering the total flow with a large amount seems to increase the stress slightly. The relation between average stress and gas ratio is shown in Figure 7.17a, and the relation between average stress and temperature is displayed in Figure 7.17b.

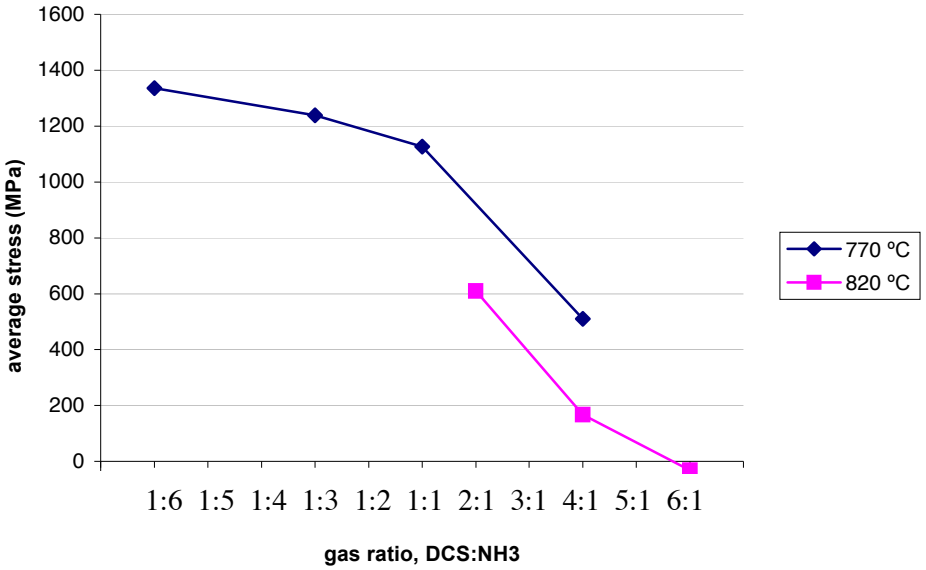

Figure 7.17a): (Above) Relation between average stress and gas ratio, at two different temperatures.

b): (Right) Relation between average stress and temperature.

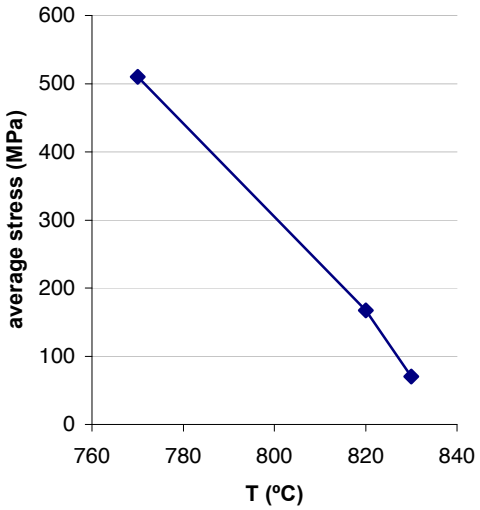

8 Discussion

To be able to come to a conclusion about the outcome of this project, a bit more background information about the demands for the silicon nitride thin film is needed. As mentioned in the introduction, section 1, the most important film properties to examine for many applications are stress and surface roughness. For most applications, low stress and low roughness are desired properties, even though there are some known situations where a high stress is useful. Maybe there could also be some situations where a high roughness is desired. Even so, this discussion will focus on applications that involve bonding processes, like in MEMS processing. Therefore, in this discussion, an optimal silicon nitride layer will have low stress and low roughness.

If the stress in the nitride film is too high, there is a risk that it will crack, and if the surface is not smooth enough the wafers will be prevented from attaching to each other with sufficient bonding force. But what kind of stress and roughness are acceptable? For stress, a clear limit is difficult to determine. Of course, a stress of a few hundred MPa indicates a much larger chance of successful bonding than values in the GPa range.

For roughness, the situation is a bit more complicated, although some indications of acceptable values can be found. One paper states that silicon wafers with a R_a value higher than 1.0 nm exhibit a significant drop in bond quality and an increase in the number of wafer voids [P1]. For pure silicon films it could be acceptable to have a RMS roughness up to approximately 2 nm. With this kind of roughness, a silicon film could still be useful for bonding applications. Silicon nitride, on the other hand, is less reactive, which means that it does not develop such strong bonding force. Therefore, it cannot be used for bonding applications at the same RMS roughness limit as pure silicon films. Instead, a RMS roughness value of perhaps 1 nm is more likely to be the limit in the case of silicon nitride.

But an exact acceptable roughness value is difficult to determine. Not only because of this uncertainty in RMS value, but also because this value does not reveal all necessary information. An explanation of this was given in section 4.2. In short, the RMS value only gives the average value of the variations in the topography of an AFM scan. Therefore, a surface with many small spikes and a surface with a few very larges spikes could show about the same RMS value. In other words, a surface that seems to have an acceptable RMS roughness value could still be useless for a bonding application because of a few large spikes on the surface, not apparent from the RMS value.

So, how does this apply to the deposited silicon nitride films from this project? A look back at the obtained stress values in Figure 7.16 shows a fairly high tensile stress throughout the first 7 runs. Another look back, but this time to Figure 7.10, shows an acceptable RMS roughness for the first 5 runs. For the sixth run it is not necessary to take PSD into consideration. Figure 7.15 has already clearly shown spikes too high to be representing a useful film. Altogether, this shows that it was difficult to obtain a film with the desired properties, since none of the films from these runs qualifies.

The question now is how these results can be used for creating a film as close to the desired properties as possible. This is important not only for stress and roughness, but also for refractive index and variations in thickness over the wafer. The evaluation from section 7 confirms the general indications of how properties are affected by different deposition

parameters, which were the original basis on which the experimental matrix was constructed. These indications are presented here together with some new conclusions.

- *High refractive indices indicate a silicon rich film*. Figure 7.3a shows clearly that this is correct. The refractive index is usually between 1.8 and 2.2, with 2.0 being the ideal value. For a DCS:NH_3 ratio of 4:1, the index resides around the limit of the given interval, i.e. around 2.2. For a ratio of 6:1 it is clearly out of range. For optical applications, a normal refractive index is very important.

- *A silicon rich film also indicates a lower tensile stress*. The more common value of a few GPa is shown for the first runs, i.e. up to a DCS:NH_3 ratio of 1:1, in Figure 7.17a. In Figure 7.17b it is shown that a high temperature reduces the stress. So, the combination of a high ratio and a high temperature is most effective for reducing stress.

- *Higher roughness with increasing temperature*. This is shown in Figure 7.11. The first 5 runs show a very low RMS roughness in Figure 7.10. It is difficult to compare the other RMS values, but some additional information can be given through the PSD graphs of Figure 7.12 and 7.13. A general conclusion is that all wafers showed a very similar roughness distribution.

- *Increasing temperature also indicates increasing variations in thickness*. From Figure 7.7a this is confirmed, but Figure 7.7b also shows a strong influence of pressure, higher pressure increases the variations in thickness.

- *Higher deposition rate with higher total flow*. That this statement is true is seen in Figure 7.5a. For the range here, between a total flow of 160 sccm and 420 sccm, the influence is not that large. Instead, deposition rate seems to be depending upon all deposition parameters, with highest value for a ratio of 1:1 in combination with high temperature and high pressure (Figure 7.5b,c,d).

Together, these evaluations give indications on how to create a film with the desired properties. Although a high deposition rate is desired, a lower value could perhaps be accepted if, at the same time, a silicon nitride layer with other very good qualities is produced. Therefore, in creating an ideal film for bonding applications, the influence of deposition parameters to deposition rate will not be considered at first. Instead, the considerations will begin with roughness, since this gives very important limitations. The strongest conclusion from the obtained results is that a low temperature together with a low gas ratio is necessary. An interesting combination would be a gas ratio of 2:1 in combination with a temperature of 770 °C. This immediately gives a problem regarding stress. Either the temperature has to be raised, or the gas ratio has to be higher. Most effective is a higher gas ratio, and the roughness would definitely increase with increasing temperature. Perhaps the temperature could be raised to 790 °C, but this would hardly have any effect on the stress. A possible, although risky (from a roughness point of view), combination would be a gas ratio of 3:1 in

combination with a temperature of 770 °C. For these parameters, the refractive index would still be in the desired interval, between 1.8 and 2.2. What about uniformity? The low temperature is desired, together with a low pressure, say 150 mTorr. This low pressure would also lower the stress slightly.

Finally, there is the issue of deposition rate. With a ratio of 3:1, low pressure and low temperature, the deposition rate would be quite low. A way to try to raise the deposition rate would be to increase the total flow. There is a recommendation regarding the furnace used here, not to use a DCS flow over 150 sccm (because of particle generation). With a DCS:NH_3 ratio of 3:1, this would mean a NH_3 flow of 50 sccm, hence a total flow of 200 sccm.

In conclusion, one suggestion of deposition parameters is:
T = 770 °C, p = 150 mTorr, DCS:NH_3 ratio = 3:1, total flow = 200 sccm.
Most likely, though, is that these conditions would create a film with high roughness.

9 Conclusions

Evaluation of the silicon nitride films deposited in this work confirms the expected general indications of how surface properties are affected by different deposition parameters.

By using a wide range of process conditions and evaluating the results obtained in each run, some conclusions about the possibility to create a thin film with low stress and low roughness could be made. Based on the results here, the most important conclusion is that an ideal combination of deposition parameters is very difficult to find. Therefore, one way to approach this problem, when making a deposition for a specific application, is to really consider what kind of stress that would be acceptable. Of course, stress and roughness can be considered equally important. Even so, a low roughness is truly a crucial property for bonding applications.

References

Books

[B1] Sze, S.M. (2002). *Semiconductor devices, Physics and Technology.* (2.ed.) John Wiley & Sons, Inc. ISBN 0-471-33372-7.

[B2] Jaeger, Richard C. (1993). *Introduction to microelectronic fabrication*. Addison-Wesley Publishing Company, Inc. ISBN 0-201-14695-9.

[B3] Campbell, Stephen A. (2001). *The Science and Engineering of Microelectronic Fabrication*. Oxford University Press, New York. ISBN 0-19-513605-5.

[B4] Wasa, Kiyotaka, et al. (2004). *Thin Film Materials Technology – Sputtering of Compound Materials.* William Andrew Publishing, Norwich, N.Y. ISBN 0815514832 (electronic bk.)

[B5] Pierson, H.O. (1999). *Handbook of Chemical Vapor Deposition – Principles, Technology and Applications* (2.ed.) Noyes Publications, Norwich, N.Y. ISBN 1591240301 (electronic bk.)

[B6] Pettersson, Leif, et al. (2004). *Ellipsometry, An introduction to laboratory work in Analytical Methods in Materials Science.* Department of Physics and Measurement Technology, Linköping University.

[B7] Arwin, Hans. (2000). *Thin film optics.* Department of Physics and Measurement Technology, Linköping University.

[B8] *Guide to Using WVASE32.* J.A. Woollam Co., Inc.

[B9] (2000). *Scanning Probe Microscopy Training Notebook.* Digital Instruments, Veeco Metrology Group.

[B10] *NanoScope Command Reference Manual, Version 4.42*. Digital Instruments.

[B11] *KLA-Tencor P-15 User's Guide for Software*, Version 6.4.

Papers

[P1] Abe, T., Matlock, J.H. *Wafer Bonding Technology for Silicon-on-Insulator Technology*. Solid State Technology. 33 (1990) 11:39.

[P2] Fang, S.J. et. al. *Analyzing atomic force microscopy images using spectral methods*. J. Appl. Phys. 82 (1997) 12.

[P3] Miller, Eric. *Low stress silicon nitride process development*. Washington Technology Center. 10/31/01.

[P4] Olson, James M. *Analysis of LPCVD process conditions for the deposition of low stress silicon nitride. Part I: preliminary LPCVD experiments*. Materials Science in Semiconducting Processing 5 (2002) 51-60.

[P5] French, P.J. et. al. *Optimization of a low-stress silicon nitride process for surface-micromachining applications*. Sensors and Actuators A 58 (1997) 149-157.

[P6] Liu, Xue-Jian, et. al. *Growth and properties of silicon nitride films prepared by low pressure chemical vapor deposition using trichlorosilane and ammonia*. Thin Solid Films 460 (2004) 72-77.

Internet

[I1] http://www.timedomaincvd.com/CVD_Fundamentals/films/SiN_thermal_CVD.html 2005-11-01

[I2] http://www.timedomaincvd.com/CVD_Fundamentals/films/SiN_plasma_CVD.html 2005-11-01

[I3] http://microtechnology.llnl.gov/Technology.html 2005-10-14

[I4] http://www.njit.edu/v2/MRC/proj13.html 2005-10-14

[I5] http://www.flipchips.com/tutorial22.html 2005-10-01